1 **TITLE**

2 *Arabidopsis thaliana* natural variation in temperature-modulated immunity uncovers
3 transcription factor UNE12 as a thermoresponsive regulator

4 **AUTHORS**

5 Friederike Bruessow[1], Jaqueline Bautor[1], Gesa Hoffmann[1,2] and Jane E. Parker[1*]

6 [1] Department of Plant-Microbe Interactions, Max-Planck Institute for Plant Breeding
7 Research, Carl-von-Linné-Weg 10, 50829 Cologne, Germany
8 [2] (Current address) Department of Plant Biology, Uppsala BioCenter, Swedish University of
9 Agricultural Sciences (SLU), 75007 Uppsala, Sweden
10
11 [*]Correspondence and requests for materials should be addressed to Jane E. Parker
12 (parker@mpipz.mpg.de)
13
14 Authors declare there are no competing interests
15

16 ## Abstract

17 Temperature impacts plant immunity and growth but how temperature intersects with
18 endogenous pathways remains unclear. Here we uncover variation between *Arabidopsis*
19 *thaliana* natural accessions in response to two non-stress temperatures (22°C and 16°C)
20 affecting accumulation of the thermoresponsive stress hormone salicylic acid (SA) and plant
21 growth. Analysis of differentially responding *A. thaliana* accessions shows that pre-existing
22 SA provides a benefit in limiting bacterial pathogen infection at both temperatures. Several *A.*
23 *thaliana* genotypes display a capacity to mitigate negative effects of high SA on growth,

indicating within-species plasticity in SA - growth tradeoffs. An association study of temperature x SA variation, followed by physiological and immunity phenotyping of mutant and over-expression lines, identifies the transcription factor *unfertilized embryo sac 12* (*UNE12*) as a temperature-responsive SA immunity regulator. Here we reveal previously untapped diversity in plant responses to temperature and a way forward in understanding the genetic architecture of plant adaptation to changing environments.

Introduction

Analysis of phenotypic variation is a means to identify genes and networks underlying complex traits[1]. Environment shapes plant phenotypes and is a driver of adaptation to new habitats[2, 3, 4]. Temperature, as one key environmental variable, impacts plant physiology, growth and responses to abiotic and biotic stresses[5, 6]. As temperature fluctuations across the globe increase, it is important to determine how plants integrate temperature signals with plant developmental and stress programs, and the genetic networks enabling resilience to climate change.

There has been recent progress in elucidating processes that coordinate temperature with plant endogenous pathways. Phytochromes act as thermosensors, coupled with their central integrative role in light quality perception and signalling[7, 8, 9]. In *Arabidopsis thaliana*, phytochrome B (phyB) regulates the bHLH transcription factor phytochrome interaction factor4 (PIF4) to prioritize growth over immune responses at elevated temperatures[10]. In the cold, membrane-bound NAC transcription factor NTL6 is released to induce disease resistance[11]. Therefore, temperature signals influence transcriptional regulation of immunity and growth.

Coordination between temperature and plant resistance to pathogen infection is determined by phytohormone pathways with contrasting roles in growth and defence, and by temperature effects on *in planta* microbial metabolism and infectivity[6, 12, 13, 14, 15]. In *A. thaliana*, the two major protective layers against microbial pathogens: cell surface-based pattern-triggered immunity (PTI) and intracellular effector-triggered immunity (ETI) respond differently to ambient temperature, with PTI being preferentially activated at elevated and ETI at lower temperatures[14, 16, 17]. Gradual depletion of the alternative histone H2A.Z in nucleosomes with increasing temperature[18] is associated with increased PTI-dependent gene expression at the expense of ETI[16]. Hence, temperature effects registered at the chromatin are also important for plant immunity outputs.

The plant stress hormone, salicylic acid (SA), mediates basal and systemic immunity to biotrophic and hemi-biotrophic pathogens by reprogramming cells for defence via the transcriptional co-regulator, nonexpressor of *PR1* (NPR1)[19]. In *A. thaliana*, pathogen-induced SA is generated mainly by the isochorismate synthase1 (ICS1) pathway [20]. Induced *ICS1* expression and pathogen resistance in *A. thaliana* basal and ETI responses are compromised at temperatures above 23-24^{o}C [5, 13, 21]. In *A. thaliana* accession Col-0, increased SA was also responsible for plant stunting after shifting from 23^{o}C to near chilling conditions (5^{o}C)[22]. Exposure of other *A. thaliana* accessions to 10°C revealed genotype-specific expression patterns for ~75% cold-regulated transcripts[23], highlighting the extent of natural variation in temperature-modulated gene expression.

Lower temperatures (<16^{o}C) amplify pathogen-activated ETI and autoimmune responses (- the latter often due to mis-activated ETI receptors) accompanied by increased SA production and pathogen resistance[17, 21, 24, 25, 26, 27, 28]. Plant autoimmune backgrounds exhibit stunting and leaf necrosis as negative consequences of activated defences on plant fitness[5]. Defence -

growth tradeoffs appear to be mainly hard-wired through phytohormone and transcriptional networks[29, 30, 31, 32], probably to steer the plant through stressful periods[33, 34]. However, there are instances in which antagonistic interactions between stress and growth pathways are uncoupled [32, 34, 35, 36, 37, 38], indicating genotypic and phenotypic plasticity in defence - growth coordination.

Here we investigate *A. thaliana* natural genetic variation in immunity responses to two temperature regimes (22/20°C and 16/14°C). Our aim was to assess the phenotypic space in immunity x growth interactions over a non-stress temperature range for this species. Using SA accumulation in leaves of 105 genetically diverse accessions as a first proxy for defence homeostasis, we uncover variation in temperature modulation of SA and in the relationship between leaf SA and biomass. At both temperatures, there is a measurable benefit of high initial SA levels on plant post-stomatal resistance to a leaf-infecting bacterial pathogen, *Pseudomonas syringae* pathovar *tomato* DC3000 (*Pst DC3000*). A genome-wide association study of temperature x SA variation identifies bHLH transcription factor *unfertilized embryo sac 12* (*UNE12*) as a new thermoresponsive immunity component.

Results

SA chemotyping of *A. thaliana* plants at two temperature regimes

To measure temperature-modulated SA accumulation we selected 105 *A. thaliana* accessions from the HapMap population based on genetic diversity and geographical distance[39]. Most accessions (80%) originate from Eurasia populations and we included naturalized lines from America, Africa, New Zealand and Japan (Table S1). Individual plants were grown in separate pots to avoid competition/shading and, as a randomized design in controlled cabinets, kept at 16°C/14°C or 22°C/20°C and 12 h light/dark cycle within the non-stress range for *A.*

thaliana[40]. We then determined biomasses and SA contents of 5-week-old plants under each temperature regime. Because there was a strong correlation between fresh and dry plant weights (Table S2), we used above-ground fresh weight (FW) as a measure of biomass.

To quantify SA in a large number of samples, we used a high-throughput SA biosensor-based luminescence method[41, 42] (Methods). This provided total SA measurements in medium (Ws-0 and Col-0) and high SA (C24 and Est-1) accumulating accessions [35, 43] with an accuracy comparable to GC-MS (Fig. S1a). The biosensor method was less reliable for quantifying low levels of free SA, the biologically active form (Fig. S1b) [44]. There was a high correlation between free and total SA amounts in GC-MS assays of 15 tested 5-week-old accessions with contrasting SA contents at 22°C (Fig. S2). We therefore used biosensor-based total SA as a measure of SA accumulation at the two temperatures. As plant age influences SA accumulation and outputs[34], we assessed whether differential SA accumulation between accessions is captured reliably at 5 weeks. For this, total SA was quantified in five accessions which in pilot studies had shown low (Sha, Col-0), intermediate (Est-1) or high (An-1) total SA contents, together with a Col-0 *isochorismate synthase* SA biosynthesis mutant *sid2-1*[20], over a 7-week time course. Total SA accumulation trends seen in 5-week-old plants persisted over the course of development from 4-7 weeks regardless of flowering time (Fig. S3).

Genetic variation in *A. thaliana* SA - growth tradeoffs

At each temperature there was considerable genetic variation in plant biomass and total SA levels between accessions (Fig. 1a and 1b, Table S1). Surprisingly, total SA did not show a general tendency to increase in plants grown at 16°C compared to 22°C, although biomasses at 16°C were lower (Fig. 1a-c). Therefore, increased SA at cooler temperatures reported previously for accession Col-0[11, 22], and also found here for Col-0 (Table S1), appears not to be generalizable for *A. thaliana*. Moreover, comparing total SA contents with biomass in each

accession revealed that at 16°C and 22°C there was an extremely weak negative correlation between total SA levels and above ground FWs (Fig. 2a and 2b). One third of accessions with total SA contents >1 µg/g FW had biomasses above the median at each temperature, suggesting that there is within-species genetic and/or phenotypic plasticity in SA - growth tradeoffs.

Negative effects of defence on growth in high SA backgrounds might be mitigated by imposing a higher induction threshold for SA immunity. We therefore measured expression of the SA-responsive *pathogenesis-related1* gene (*PR1*) at 22°C in selected 5-week-old accessions with high total SA amounts (>1 µg/g FW) and high biomass (>1.5 g) (Ven-1, PHW-13, Kas-2), accessions with high total SA and low biomass (>0.5 g) and some leaf necrosis (Gy-0, Spr1-2, Mz-0), or with low total SA (<0.3 µg/g FW) and varied biomass (Mrk-0, Col-0, Oy-0) (Fig. 2c-f). For these nine tested accessions, high total SA was accompanied by elevated *PR1* expression but not always stunting (Fig. 2c-f). The data suggest that mechanisms other than responsiveness to SA reduce antagonism of growth in some *A. thaliana* genetic backgrounds.

SA accumulation in response to temperature is genotype-specific

Because SA amounts in leaves of different accessions did not relate strongly with reduced growth, we examined temperature effects on SA homeostasis regardless of biomass. From the initial 105 *A. thaliana* accessions, we selected lines that accumulated higher total SA at 22°C than 16°C (Ven-1, Mz-0, Nok-3), lines that showed no variation in total SA levels between the two temperatures (Se-0, NFA-8), and lines displaying higher total SA at 16°C than at 22°C (Fei-0, Ei-0, Bay-0, Est-1) (Table S1 and Fig. 3a). Reference accessions Col-0 and Ler-0 had relatively small but opposing total SA responses to temperature (Table S1 and Fig. 3a).

We concluded that even a moderate change in temperature within the normal range of *A. thaliana* (here 6°C) exposes variation in SA pathway homeostasis.

Temperature-modulated SA impacts bacterial pathogen growth in leaves

With differences of up to 5 µg total SA/g FW in accessions grown under the two temperature regimes (Fig. 1c), we anticipated temperature-dependent variation in immune responses between accessions, as suggested by the *PR1* expression profiles of selected genotypes at 22°C (Fig. 2e). We spray-inoculated leaves of the 5-week-old accessions showing diverse total SA levels at 16°C and 22°C (Fig. 3a) with virulent *Pst DC3000* at these two temperatures. *Pst* DC3000 produces the JA-Ile mimic coronatine (COR) which promotes reopening of leaf stomata to counter bacterial PAMP-induced stomatal closure and increase bacterial entry to the leaf apoplast[15]. Host-produced SA induces stomatal closure and post-stomatal resistance to *Pst* DC3000[15, 45, 46]. At 3 h post inoculation (hpi), *Pst* DC3000 levels inside leaves were unchanged between temperatures in each accession but showed up to 10-fold differences between accessions (Fig. S4a). We therefore excluded stomatal resistance as contributing significantly to the temperature effects observed on bacterial infection in these 11 accessions. After measuring *Pst* DC3000 growth in leaves of plants at 4 dpi, we found a robust inverse correlation between temperature-modulated total SA accumulation and bacterial growth across accessions (Fig. 3b). Thus, in accessions showing a rise in total SA between 16°C and 22°C there was increased resistance to *Pst* DC3000 and the opposite trend was observed in plants which had reduced total SA between 16°C and 22°C (Fig. 3b). Accessions which responded negligibly to temperature at the level of SA accumulation showed no difference in temperature effects on *Pst* DC3000 infection (Fig. 3b). These data reveal a positive relationship between temperature-modulated total SA accumulation and post-stomatal limitation of *Pst* DC3000 growth in leaves of the 11 tested *A. thaliana* accessions.

We observed variation between accessions in the degree to which total SA differences impacts bacterial resistance. For example in Ler-0, a rise of only 0.38 µg/g FW total SA between 16°C and 22°C resulted in a substantial (1.5 $\log_{10}$) reduction in bacterial numbers (Fig. 3b). Est-1, with a much higher total SA differential (1.68 µg/g FW) between temperatures, showed only a small (0.5 $\log_{10}$) difference in bacterial growth, whereas in Fei-0 a 2.56 µg/g FW total SA change translated to a 2.0 $\log_{10}$ bacterial growth difference (Fig. 3b). All accessions in Fig. 3 had proportional free and total SA levels (Fig. S2). Together, these data suggest there is variation between *A. thaliana* accessions in the extent to which accumulated SA translates to bacterial immunity. When cultured on liquid M9 minimal salt medium containing sorbitol as carbon source over a 56 h time course, *Pst DC3000* grew more slowly at 16°C than at 22°C during the exponential phase (Fig. S5). This result emphasizes the influence of *A. thaliana* host genotype in determining temperature effects on post-stomatal bacterial growth in leaves.

High SA accumulation prior to infection increases bacterial immunity

We have shown that *A. thaliana* SA amounts before infection correlate positively with resistance to virulent *Pst* DC3000. Next we tested whether temperature effects on *Pst* DC3000-induced SA might also contribute to resistance in these accessions. For this, leaves of accessions Ven-1, Mz-0, Fei-0, Ei-2, Col-0 and Se-0 grown at 16°C or 22°C were sprayed with *Pst* DC3000 or buffer (mock) and total SA measured at 24 hpi. Similar temperature effects on total SA accumulation were observed in these accessions after mock treatment as in untreated plants (compare Fig. 4 (mock) and Fig. 3a). After *Pst* DC3000 inoculation, there were no significant temperature differences in total SA accumulation between accessions (Fig. 4). Hence, accessions with lower starting (basal) SA at 16°C or 22°C induced SA to comparable levels as high initial SA accumulators at 24 hpi (Fig. 4). We concluded that

temperature modulated SA accumulation before infection is an important determinant of *A. thaliana* immunity to *Pst* DC3000 bacteria.

SA underlies differential temperature effects on resistance to bacteria

We tested whether the observed temperature-dependent differences in bacterial resistance between accessions are determined by SA levels. For this, we introduced into different *A. thaliana* accessions a bacterial *NahG* (*salicylate hydroxylase*) gene which breaks down SA to catechol[47]. A single *NahG* transformant line from each accession was selected after checking total SA depletion at the temperature the parental accession produced highest SA amounts (Fig. S6). The SA-depleted (*NahG*) accessions, together with existing Ler-0 and Col-0 *NahG* lines[48, 49] grown at 16°C or 22°C, were spray-inoculated with *Pst DC3000* and bacterial titers measured in leaves at 3h and 4 dpi. There was again no detectable temperature effect on *Pst* DC3000 stomatal entry to leaves at 3 hpi (Fig. S4b). In contrast to the parental responses (Fig. 3b), corresponding *NahG* lines had lost temperature-dependent differential resistance to *Pst* DC3000 growth at 4 dpi (Fig. 3c). This loss was also observed in Col-0 *sid2-1* (Fig. 3c). These data suggest that temperature-regulated SA accumulation directly or indirectly underlies the observed temperature effects on resistance to virulent *Pst* bacteria, and that the isochorismate SA biosynthesis pathway is sensitive to the temperature range used here.

Notably, variation in *Pst* DC3000 growth between wild-type accessions persisted in the corresponding *NahG* transgenic lines that was independent of temperature (Fig. 3b,c). For example, up to a 1000-fold difference in *Pst* DC3000 titers was observed between the most susceptible (Nok-3 and Ler-0) and resistant (Mz-0 and Ei-2) genotypes (Fig. 3c). These data highlight a substantial contribution of SA-independent processes in limiting *Pst* DC3000 growth which, unlike the SA-dependent resistance, are unaffected by changes in temperature within the 16°C to 22°C range. We concluded that there is within-species genetic variation in

229 both temperature-dependent SA and temperature-independent (non-SA) defences shaping *A.*
230 *thaliana* post-stomatal immune responses to bacteria.
231
232 **Genetic architecture of SA regulation by temperature in *A. thaliana***
233 After assessing SA homeostasis in response to temperature in 105 *A. thaliana* accessions, we
234 examined whether specific phenotypes fit a global distribution pattern, using the coefficients
235 of a GLM (Generalized Linear Model; Materials and Methods) to colour-code phenotypes at
236 occurrence sites. There were no obvious geographic or climatic distribution patterns found for
237 temperature-dependent total SA regulation (Methods) (Fig. 5a; representing only extended
238 European accessions for clarity).
239
240 Broad sense heritability of SA accumulation was calculated to be 0.79 at 16°C and 0.76 at
241 22°C, indicating a sizable genetic underpinning to this trait. To explore the trait genetic
242 architecture we performed temperature x total SA association mapping on 99 accessions using
243 the GWAPP tool[50] and coefficients of the GLM as a phenotype (Methods). One major peak
244 on the upper arm of chromosome 4 contained six significant single nucleotide polymorphisms
245 (SNPs) after Bonferroni multiple testing correction (Fig. 5b and Table S3). Two additional
246 peaks were found on chromosomes 1 and 4, each with one significantly associated SNP after
247 Bonferroni correction (Fig. 5b and Table S3). Immediate and neighbouring genes within 10
248 kb each side of the significant SNPs were considered as candidates (Table S3)[51]. Two SNPs
249 on the upper arm of chromosome 4 fall in the bHLH transcription factor gene *unfertilized*
250 *embryo sac 12 (UNE12*), in which a T-DNA insertion in Col-0 led to slightly increased
251 resistance to a virulent strain of the oomycete pathogen *Hyaloperonospora arabidopsidis*[52].
252 None of the six remaining significant SNPs considered by the GWAPP tool was in a gene
253 related to SA biosynthesis/signalling, temperature responses, defence or cell death regulation
254 (Table S3) except for *At4g02600,* a homologue of barley *mildew resistance locus O1*

(*ATMLO1*)[53]. However, *ATMLO1* expression was found to be specific to early development[53]. In the GWAS analysis, *A. thaliana* genes involved in thermosensory regulation, such as *PIF4*, *PhyB*, *NTL6* or genes controlling alternative histone H2A.Z recruitment [7, 10, 11, 18], were not found to be associated with temperature-dependent SA regulation. Because Bonferroni is conservative, we extended the list of candidate genes in the vicinity of SNPs with a reduced significance level of –log(P) = 5.5 (Table S3). This identified SCF E3 ubiquitin ligase complex genes: *Skp1 interacting protein5* (*SKIP5*), *cullin1* (*CUL1*), two *F-Box protein* genes (*At3g25750, At3g54460*) and a *ubiquitin ligase protein degradation gene* (*At3g29270*) as candidates for temperature-dependent SA regulation (Table S3). Several other candidates are associated with transcription (*UNE12*, *RNA polymerase II E*, transcription factor *At2g46510* and transposable elements (*TE*) (Table S3).

Comparison of *UNE12* functions with thermosensory immune regulator *PIF4*

As *UNE12* is supported by two significantly associated SNPs on chromosome 4 (Fig. 5b,c and Table S3), we investigated its role in temperature-dependent SA accumulation and immunity. Using TAIR.10 sequence data to identify *UNE12* genomic polymorphisms with the Col-0 reference genome (http://signal.salk.edu/atg1001/3.0/gebrowser.php) we examined sequences from accessions with extreme or intermediate temperature x SA phenotypes that were also used for the *Pst* DC3000 infection assays (Fig. 3). Variation was uncovered in *UNE12* coding and regulatory sequences (Fig. 5c). While accessions Bay-0 and Se-0 have several deletions and nucleotide exchanges in the *UNE12* coding sequence relative to Col-0, all other considered accessions only display one SNP in the coding sequence (Fig. 5c). Since this SNP leads to a synonymous mutation, we reasoned that variation in expression of *UNE12* rather than protein sequence might underlie temperature-modulated SA and/or bacterial resistance.

A T-DNA line with an insertion in the last intron of *UNE12* leading to a truncated transcript (SALK_13303; *une12-13* - verified by qRT-PCR (Fig. 6a and Table S4)), and a β-estradiol inducible *UNE12* transgenic line (*βE::UNE12*) from the TRANSPLANTA Col-0 collection[54], were selected for phenotyping. Because the bHLH TF *PIF4* and its closest homologue *PIF5* are temperature-sensing immunity regulators under control of the PhyB thermosensory pathway in Col-0[10], we explored redundancy or cooperativity between *PIF4/PIF5* and *UNE-12* by including the *pif4-2 pif5-3* double mutant and a *PIF4::PIF4HA pif4-101* over-compensating transgenic line[55, 56] in our assays. In 5-week-old Col-0 plants at 16°C, *UNE12* expression was low and increased 0.5-fold at 22°C (Fig. 6a). As expected, *une12-13* had no detectable full-length transcript whereas the estradiol-untreated *βE::UNE12* line expressed 2-fold higher *UNE12* than Col-0 at both temperatures (Fig. 6a). *PIF4* expression was undetectable in *pif4-2 pif5-3* and was elevated in the *PIF4::PIF4HA pif4-101* line at 16°C compared to Col-0, and further boosted in *PIF4::PIF4HA pif4-101* leaves at 22°C (Fig. 6b). Loss or gain of *PIF4* expression, respectively in *pif4-2 pif5-3* and *PIF4::PIF4HA pif4-101*, did not alter *UNE12* expression at either temperature (Fig. 6a). Reciprocally, *PIF4* expression which was higher than *UNE12*, did not change within the 6°C temperature range in Col-0 or *une12-13* and *βE::UNE12* lines (Fig. 6b). Therefore, *UNE12* and *PIF4*/*PIF5* do not influence each other's expression under the tested conditions.

UNE12 has features of a temperature-responsive immunity regulator

We quantified total SA in the above lines at 16/14°C and 22/20°C. Col-0 SA levels decreased with increased temperature (Fig. 6c) as observed before (Fig. 3a). At 16°C, the *une12-13* mutant had similar total SA amounts as Col-0 but, unlike Col-0, maintained the same SA level at 22°C (Fig. 6c). Strikingly, 2-fold over-expression of *UNE12* in the *βE::UNE12* line led to low total SA accumulation at both temperatures (Fig. 6c). Therefore, mis-regulation of *UNE12* alters SA accumulation in response to temperature. We found that *pif4-2 pif5-3* did

not alter temperature modulation of total SA but that *PIF4* over expression (in *PIF4::PIF4HA pif4-101*) reduced total SA in plants grown at 16°C and further at 22°C (Fig. 6c). These data suggest that *UNE12* and *PIF4* operate differently in transmitting temperature information to SA accumulation.

Next we tested whether the temperature x SA profiles in the above lines tally with changes in SA-based immunity by quantifying *PR1* expression and *Pst* DC3000 growth in 5-week-old plants at 16°C and 22°C. *PR1* expression and resistance to *Pst* DC3000 correlated with SA regulation by temperature in these lines with two exceptions (Fig. 6c-e). At 22°C, *PR1* expression in *une12-13* was lower than expected based on its SA accumulation and resistance to *Pst* DC3000 (Fig. 6c-e). By contrast, the *PIF4* overexpression line (*PIF4::PIF4HA pif4-101*) exhibited equivalent low SA and *PR1* expression but higher *Pst* DC3000 susceptibility than Col-0 at 22°C (Fig. 6c-e). At 3 hpi, *Pst DC3000* bacterial entry was similar between temperature regimes and lines (Fig. 6f), suggesting that the observed *UNE12* and *PIF4* effects on bacterial resistance are mainly post-stomatal. Taken together, these data suggest that *UNE12* participates in temperature regulation of SA immunity and do not support a conjunction of *UNE12* and *PIF4* pathways in this temperature response.

UNE12 mis-regulation does not alter _A. thaliana_ development

A. thaliana PIF4 has an important role in thermomorphogenesis in which it negatively regulates pathogen immunity to favour plant growth at increased temperature[6, 10]. Mis-regulation of *PIF4* and its homologues alters hypocotyl and petiole elongation, growth and onset of flowering. We therefore compared developmental phenotypes of the *une12-13, βE::UNE12, pif4-2 pif5-3*, *PIF4::PIF4HA pif4-101* lines and Col-0 after 5 weeks at 16/14°C and 22/20°C and a 12 h light/dark cycle, as in the previous assays. The *une12-13* mutant and *βE::UNE12* over expression line resembled Col-0 in stature (Fig. 7a). By contrast, *pif4-2 pif5-*

3 plants were stunted at 22°C and *PIF4::PIF4HA pif4-101* had longer petioles (Fig. 7a), as reported[10, 55, 57]. Hypocotyl lengths were similar between *UNE12* lines and Col-0 at both temperatures, but were shorter in *pif4-2 pif5-3* and longer in *PIF4::PIF4HA pif4-101* at 16°C and 22°C (Fig. 7b)[6]. Deviations from Col-0 were also observed in above-ground FWs of the *PIF4* lines at 16°C and 22°C, but not in the *UNE12* lines (Fig. 7c). Flowering time was similar in all lines at 16°C but delayed in the *PIF4* lines at 22°C (Fig. 7d). Delayed flowering was reported for *PIF*-deficient lines grown at ~22°C, whereas *PIF* over-expressors accelerated flowering[18, 57]. Why this latter trend is not observed under our growth conditions remains unclear. Phenotypic analysis of an independent *UNE12* T-DNA insertion line (SALK_010825C; *une12-01*)[52] compared to wild-type Col-0 showed that it behaves similarly to *une12-13* at 16°C and 22°C at the level of *UNE12* and *PR1* expression, total SA accumulation and plant biomass (Fig. S7a-e). These data lead us to conclude that *UNE12* expression in *A. thaliana* Col-0 impacts temperature modulation of SA immunity without markedly altering developmental traits and that *UNE12*-related thermosensory processes affecting SA accumulation and immunity to *Pst* DC3000 are distinct from those controlled by *PIF4*.

Discussion

Here we explored *A. thaliana* natural variation in response to temperature impacting SA accumulation, growth and resistance to bacterial (*Pst* DC3000) infection. One aim was to determine differential temperature effects on immunity within a non-stress range, taking SA as an initial proxy for plant defence status. A second aim was to identify potential benefits and costs of accumulating high or low SA at a particular temperature. By testing 105 genetically diverse *A. thaliana* accessions, we uncover variation in total leaf SA accumulation between the 16°C and 22°C temperature regimes. We establish that increased SA amounts do not always correlate with reduced biomass, indicating a capacity of certain *A. thaliana* genotypes

to mitigate negative effects of high SA levels on growth. Using a set of 15 selected accessions covering the range of observed temperature-modulated SA and growth responses, we detect a robust positive relationship between total SA in leaves prior to infection and post-stomatal restriction of *Pst* DC3000 growth, representing a possible benefit of accumulating SA. From an association study of temperature x SA in 99 of the 105 accessions, we identify *UNE12* as a strong candidate for thermoresponsive control of SA immunity to *Pst* DC3000. This analysis uncovers diversity in plant responses to temperature and a way forward to understand the genetic architecture of plant adaptation to changing environments.

We were able to group *A. thaliana* accessions into three broad classes based on increased, decreased or stable total SA contents associated with the 16°C - 22°C temperature difference (Fig. 1c, Fig. 3a). *A. thaliana* Col-0, the most studied accession for temperature effects on immunity and growth[13, 14, 21, 22, 24, 58], showed a comparatively weak negative SA accumulation trend with increased temperature (Fig. 3a, Fig. 6c). In a previous study, higher SA in Col-0 plants grown at 5°C compared to 23°C contributed to growth retardation at the chilling temperature[22], consistent with tradeoffs between induced plant defences and growth[29, 32].

A. thaliana autoimmunity phenotypes leading to growth inhibition and necrosis have been linked to increased SA[17, 25, 26, 27]. It is therefore striking that ~ 33% of the 105 accessions with >1µg/g FW total SA retained a biomass above the median of the tested genotypes (Fig. 2a-b). That certain accessions with high SA exhibited increased resistance to *Pst* DC3000 or *PR1* expression without a measurable biomass penalty (eg. Ven-1, Kas-2, PHW-13 in Fig. 2c-e and Fig. 3a-b), points to genotypic variation in the threshold at which SA leads to autoimmunity[23]. Presence of genetic modifiers of SA-related autoimmunity and stress sensitivity are evident from studies of different *A. thaliana* accessions[35, 59]. Alterations in the hormone network controlling SA crosstalk with growth-promoting pathways might buffer against SA negative

384 effects in some genotypes[60]**.** Notably, SA signalling contributes positively to petiole
385 elongation in the *A. thaliana* Col-0 shade avoidance growth response [61]. Also, defences and
386 growth were effectively uncoupled in *A. thaliana* Col-0 in a *Jasmonate-Zim Domain* (*JAZ*)
387 repressor x *phyB* sextuple mutant, indicating that perturbation of the hormone transcriptional
388 network can reduce defence - growth tradeoffs [37]. *A. thaliana* accession C24 displays an
389 unusual broad-ranging tolerance to stress encounters with little negative impact on growth[62].
390 For accessions with different SA - growth relationships identified in our analysis (Fig. 2c-d),
391 it will be interesting in future studies to pinpoint underlying stress network properties and
392 whether the apparent benefit of high SA on bacterial resistance creates vulnerabilities to other
393 environmental stresses or conditions.
394
395 Phenotypic characterization of 15 differential accessions revealed a positive relationship
396 between total SA accumulation in response to temperature and post-stomatal restriction of *Pst*
397 DC3000 growth in leaves, with plants being more resistant at the temperature the respective
398 unchallenged accession accumulated higher SA (Fig. 3). SA amounts in plants within the
399 studied 6^{o}C temperature range might thus be a predictor of resistance capability. Some
400 accessions (eg. Ven-1, Nok-3, Ler-0, Fei-0) displayed more than 50-fold differences in *Pst*
401 DC3000 growth at 4 dpi between the two temperatures (Fig. 3b) which is similar to the
402 differential growth observed between virulent and avirulent *Pst* strains in leaves of *A. thaliana*
403 accessions Col-0 or Ws-2[58]. Therefore, even a moderate temperature change can have a
404 similar impact on bacterial infection as effector-triggered immunity. Quantifying *Pst DC3000*
405 titres in the corresponding *NahG*-transgenic lines showed that SA depletion abolished the
406 temperature effect on *Pst DC3000* growth in all of the tested accessions (Fig. 3). Hence, the
407 temperature effect on resistance to bacterial growth appears to be an SA-dependent trait in
408 these accessions. Huot et al (2017) established that SA signalling represents a major
409 temperature-sensitive resistance node in *A. thaliana* accession Col-0, assessed over a warmer

410 temperature range of 23- 30°C, and that high temperature suppression of immunity to *Pst*
411 DC3000 was independent of *PhyB* and *PIF4* [13]. These and our data emphasize the importance
412 of temperature differences within the normal range experienced by *A. thaliana* on
413 effectiveness of SA-based pathogen immunity.
414
415 The differences in *Pst* DC3000 titres remaining between *NahG*-expressing accessions (Fig.
416 3c), clearly expose a contribution of SA-independent processes to variation in resistance to
417 virulent bacteria, as also indicated by a screen of 1041 *A. thaliana* accessions in response to
418 spray-inoculated *Pst* DC3000[63]. High humidity levels used in that screen affected plant
419 stomatal and post-stomatal immune responses [63, 64] and might explain why Mz-0, the most
420 resistant accession in our hands (Fig. 3b), was not identified there. Mz-0 displays an
421 autoimmune phenotype at 22°C with chlorosis, stunting and high SA accumulation due to a
422 hyperactive allele at the *ACD6* locus[43]. Nevertheless, the Mz-0 *NahG* line retained strong SA-
423 independent resistance to *Pst* DC3000 (Fig. 3c). In Col-0, post-stomatal basal and effector-
424 triggered immunity to *Pst* DC3000 strains can be divided into parallel SA-dependent and SA-
425 independent resistance branches[46, 65, 66]. SA-independent resistance provides some protection
426 against pathogens that can disable SA pathways. Our and other analyses suggest that part of
427 that resilience might lie at the level of maintaining SA-independent immunity over a range of
428 temperatures[14, 16].
429
430 The differences in SA contents regulated by temperature between *A. thaliana* accessions was
431 not clearly linked to a geographical distribution pattern (Fig. 5a) and therefore it is not known
432 whether this represents an adaptive trait to local climatic conditions[67]. Loci strongly
433 associated with climate variables were enriched in amino acid-changing SNPs, indicating the
434 presence of adaptive alleles[2]. There is increasing evidence for microhabitat effects such as
435 edaphic conditions, intraspecific competition, herbivore distribution and altitude playing roles

436 in local adaptation[3, 68, 69]. A study on the genetic basis to local adaptation of *A. thaliana* in
437 Europe revealed several associated loci related to immunity[67]. Also, defence and cold
438 response processes were associated with adaptive climate variables[2]. Taken together, these
439 data suggest that temperature modulation of plant defences is likely to impact local
440 adaptation.
441
442 Association mapping allowed us to link variation in temperature-dependent total SA to three
443 loci on two chromosomes, with a strongly supported QTL on chromosome 4 (Fig. 5b). In *A.*
444 *thaliana* Col-0, *UNE12* has features of a thermoresponsive immunity component because loss
445 or mild over-expression of this gene disturbed temperature effects on SA accumulation and
446 basal resistance to *Pst* DC3000 bacteria (Fig. 6e). Interestingly, UNE12 was identified as a
447 weak negative component of Col-0 immunity and, in yeast 2-hybrid assays, as a potential
448 defence hub connected to multiple NLRs[52]. Polymorphisms in the *A. thaliana UNE12* coding
449 sequence exist but only one synonymous mutation was significantly associated with
450 temperature-modulated SA homeostasis (Fig. 5c). Third base polymorphisms do not influence
451 protein sequence but can affect translation efficiency[70]. The positions of other significantly
452 associated SNPs in *UNE12* intronic and promoter regions (Fig. 5c), together with phenotypes
453 of Col-0 misexpressed *UNE12* lines uncovered here (Fig. 6), point to *UNE12* expression
454 influencing temperature modulation of SA-based immunity. Our comparative physiology and
455 immunity phenotyping of *PIF4*/5 and *UNE12* mis-expressed lines (Fig. 6 and Fig. 7) suggests
456 that these factors act independently in transmitting or processing temperature stimuli to
457 immune and growth responses. Also, *UNE12* was not identified as a PIF4 transcriptional
458 target [71]. Therefore, in line with Huot et al (2017) findings, we think it unlikely that
459 temperature modulation of *A. thaliana* SA defences involves PIF4/5 signalling. Loss-of-
460 function *UNE12* mutations in accession Col-0 enhanced resistance to *Pst* DC3000 without an
461 obvious physiological or developmental cost at 22°C (Fig. 6e and Fig. 7). It will be interesting

462 to test whether manipulating control of *UNE12* expression is a way to optimize plant survival
463 against pathogen infection over a range of temperatures.
464

465 # Methods

466 ## Materials

467 For the temperature screen we used a sub-collection of 105 *A. thaliana* accessions from the
468 Hapmap population (http://bergelson.uchicago.edu/wp-content/uploads/2015/04/Justins-360-
469 lines.xls), provided by Maarten Koornneef (MPI for Plant Breeding Research, Cologne). This
470 population was developed from a global collection of 5810 accessions in order to reduce
471 redundancy and relatedness, which is a problem in GWA studies[72, 73]. Accessions were chosen
472 based on geographic distance and seed availability (Table S1). None of the lines required
473 vernalization to flower. *A. thaliana* transgenic lines used were: *sid2-1*[20], Col-0 *NahG*[48], Ler-0
474 *NahG*[49], Est-1 *NahG* and plasmid MT363 with the *NahG* construct[43] were provided by Detlef
475 Weigel (MPI for Developmental Biology, Tübingen). Fei-0, Ei-2, Bay-0, Ven-1, Mz-0 and
476 Nok-3 accessions were transformed with pMT363 via floral dipping as described[43]. *UNE12* T-
477 DNA insertion lines SALK_010825C (*une12-01*) and SALK_13303 (*une12-13*), and a β-
478 estradiol-inducible line[54] were obtained from Nottingham Arabidopsis Stock Centre
479 (http://nasc.nott.ac.uk) and *UNE12* expression checked via RT-qPCR (Table S3). Lines *pif4-2*
480 *pif5-3*[55] and *PIF4::PIF4HA pif4-101*[56] were provided by Christian Fankhauser (University of
481 Lausanne).

482 ## Plant growth conditions

483 *A.thaliana* plants were grown under controlled conditions at 16±1°C (day) and 14±1°C
484 (night) or 22±1°C (day) and 20±1°C (night), 60±10% relative humidity, 200µE m^2 s^{-1} light
485 intensity and 12h day/night cycle. Seeds were first stratified in soil at 4°C for 3 d. Plants were
486 grown in individual 0.8l pots with commercial potting soil pretreated with entomopathogenic

nematodes. Pots were distributed into trays in a fully randomized design for temperature x SA screening. One plant per accession was grown in each replicate. Data from three independent experiments (biological replicates) at 22°C and four at 16°C were used for analysis. Plants were grown in parallel in two growth chambers after ensuring replicability of results between chambers.

Bacterial infection and *A. thaliana* physiology assays

For *Pst* DC3000 infection assays and *UNE12/PIF4* mutant characterization, plants were distributed in trays in a randomized design by genotype row. SA and gene expression assays were performed on three plants for each genotype in three independent experiments. Bacterial entry into leaves through stomata was determined by measuring *in planta* bacterial titers at 3 hpi in a total of nine plants (with three individual plants per independent experiment). At 4 dpi, bacterial growth was determined in a total of 18 plants (derived from three independent experiments). Random groups of six genotypes were tested in parallel at each temperature with at least one wild type in each group. Trays were distributed randomly in a phytotron growth chamber and moved once a week to a new position. For spray-inoculation of 5-week-old plants with *Pst* DC3000, bacterial suspensions at 0.15 OD_{600} in 10 mM $MgCl_2$ were used, as described[74].

Bacterial growth in culture

Growth of *Pst* DC3000 (empty vector pVSP61, used for all *in planta* experiments) was assessed in 20 ml M9 minimal salt medium (per L: 100ml 10 x M9 salts, 100 µl 1 M CaCL2, 1000 µl 1M MgSO4, 25 g Sorbitol, 5g Sucrose pH 7.2 (NaOH)) with Rifampicin 40 µg/ ml, Kanamycin 25 µg/ ml, after transferring 200 ul of a 20 ml overnight culture in 5 ml LB medium (Rif 40 µg/ml, Kan 25 µg/ml). Bacteria were then grown in the dark with shaking at 200 rpm for 56 h at 16°C or 22°C and OD_{600} was measured with a photometer.

Salicylic acid measurements

Luminescence produced by induction of an SA degradation operon coupled to a LUX cassette was used to measure SA in leaves using the biosensor-based method, as described[41, 42]. Total and free SA was quantified by GC-MS as described[75]. For both methods, 100-200 mg leaf samples were frozen in liquid nitrogen and disrupted by a tissue lyzer (Retsch). Material was suspended in 250µl NaOAc 0.1M pH5.5 and mixed. Samples were centrifuged in a microfuge for 15 min, 200µl supernatants transferred to a 96 well PCR plate and treated with 4U of almond beta-glucosidase (Sigma) at 37°C for 1.5 h. For bio-sensor measurements, 30µl sample was transferred to a 96 well black optiplate (Perkin Elmer) containing 60µl LB medium. A standard curve for SA (Sigma) was used in a volume of 10µl complemented with 20µl β-glucosidase-treated leaf extract of Col-0 *NahG* leaves to mimic leaf samples. The standard curve was designed and tested to measure SA concentrations from 0 to 20 µg total SA/g leaf fresh weight. The transgenic *Acinetobacter* luminescent strain was grown as described[76] and 50 µl bacterial suspensions (OD_{600} 0.4) were added to each optiplate sample before incubating at 37°C for 1h. The optiplate was then read by a luminometer (Berthold technologies) measuring luminescence emitted by each sample in 1/3s. Mean luminescence taken from three plate readings was used to calculate total SA concentrations. Because luminescence increase in the standard curve was non-linear we interpolated the data points using the approxfun() function in R (Cran 3.2.2.).

Genome wide association study (GWAS)

Broad sense heritability of total SA contents in both temperature environments was estimated as $H^2 = \sigma^2 accession / \sigma^2 accession + \sigma^2 residuals$ based on a linear model using log^{10}-transformed total SA data for normalization. Variation in temperature-dependent total SA was expressed using the coefficients of the glm model: Total SA~accession*temperature+replicate fitted with a gamma distribution to account for variation due to temperature as well as between biological replicates. Association mapping was performed on 99 accessions using the GWAPP online application https://gwas.gmi.oeaw.ac.at/[50]. We chose to further normalize the

glm coefficients with a box cox power transformation and used the accelerated mixed model (AMM) to account for population structure[50]. SNPs were considered as significantly-associated with phenotype when they withstood Bonferroni multiple-testing correction.

Quantitative RT-qPCR

RNA was extracted from liquid Nitrogen-frozen plant material using a my-budget Plant RNA kit (Bio Budget technologies Gmbh) according to manufacturer's instructions. cDNA was synthesized from 1µg plant RNA using M-MLV reverse transcriptase (Promega) following the manufacturer's protocol. RT-qPCR was performed with IQ SYBR Green supermix (Bio Rad) on a CFX Connect Real time system (Bio Rad). RT-qPCR primer sequences are listed in Table S3. Relative expression of test genes was measured against *SAND* (*At2g28390*) as a stable reference gene[77]. Relative expression of genes was assessed in three plants per genotype, each from an independent experiment.

Statistical Analysis

We performed statistical analyses on at least three samples from three biological replicates using R package version 3.3.1. Comparison between two groups was done using a two-tailed Student t-test or non-parametric Kruskal Wallis test. Multiple comparisons were performed by one-way ANOVA and Tukey's multiple testing correction applied, except for data in Fig. 2c-e where false discovery rate was used. Raw data for Fig. 1, Fig. 2 a-d, Fig. 3a and Fig. 5a are provided in Table S1. Correlations were assessed using Pearson's product moment correlation coefficient.

Acknowledgements

We thank Jonas Klasen, Dmitry Lapin and Rubén Garrido-Oter for help with statistics and Angela Hancock (MPI for Plant Breeding Research, Cologne) and Rubén Alcázar (University of Barcelona) for constructive comments on the manuscript. Funded by The Max-Planck

Society, the Cluster of Excellence on Plant Science (CEPLAS; JEP, FB) and Swiss National Science Foundation grant PBLAP3-142776 (FB).

Author contributions

FB conceived and designed the study, collected and analyzed data and co-wrote the paper; JB generated *NahG* transgenic lines and data for Fig. S6; GH collected data for Fig. 3b; JEP conceived and designed the study, analyzed data and co-wrote the paper.

References

1. Bazakos C, Hanemian M, Trontin C, Jimenez-Gomez JM, Loudet O. New Strategies and Tools in Quantitative Genetics: How to Go from the Phenotype to the Genotype. In: *Annual Review of Plant Biology, Vol 68*, 435-455 (2017).

2. Hancock AM*, et al.* Adaptation to Climate Across the Arabidopsis thaliana Genome. *Science* **334**, 83-86 (2011).

3. Brachi B*, et al.* Coselected genes determine adaptive variation in herbivore resistance throughout the native range of Arabidopsis thaliana. *Proceedings of the National Academy of Sciences of the United States of America* **112**, 4032-4037 (2015).

4. Wagner MR, Mitchell-Olds T. Plasticity of plant defense and its evolutionary implications in wild populations of Boechera stricta. *Evolution* **72**, 1034-1049 (2018).

5. Alcazar R, Parker JE. The impact of temperature on balancing immune responsiveness and growth in Arabidopsis. *Trends in plant science* **16**, 666-675 (2011).

6. Quint M, Delker C, Franklin KA, Wigge PA, Halliday KJ, van Zanten M. Molecular and genetic control of plant thermomorphogenesis. *Nat Plants* **2**, 15190 (2016).

7. Legris M*, et al.* Phytochrome B integrates light and temperature signals in Arabidopsis. *Science* **354**, 897-900 (2016).

8. Jung JH*, et al.* Phytochromes function as thermosensors in Arabidopsis. *Science* **354**, 886-889 (2016).

598 9. Ezer D*, et al.* The evening complex coordinates environmental and endogenous
599 signals in Arabidopsis. *Nat Plants* **3**, 17087 (2017).

600
601 10. Gangappa SN, Berriri S, Kumar SV. PIF4 Coordinates Thermosensory Growth and
602 Immunity in Arabidopsis. *Current Biology* **27**, 243-249 (2017).

603
604 11. Seo PJ*, et al.* Cold activation of a plasma membrane-tethered NAC transcription factor
605 induces a pathogen resistance response in Arabidopsis. *Plant Journal* **61**, 661-671 (2010).

606
607 12. Mang HG*, et al.* Abscisic acid deficiency antagonizes high-temperature inhibition of
608 disease resistance through enhancing nuclear accumulation of resistance proteins SNC1
609 and RPS4 in Arabidopsis. *The Plant cell* **24**, 1271-1284 (2012).

610
611 13. Huot B*, et al.* Dual impact of elevated temperature on plant defence and bacterial
612 virulence in Arabidopsis. *Nature Communications* **8**, 1808 (2017).

613
614 14. Menna A, Nguyen D, Guttman DS, Desveaux D. Elevated Temperature Differentially
615 Influences Effector-Triggered Immunity Outputs in Arabidopsis. *Frontiers in plant science*
616 **6**, 995 (2015).

617
618 15. Xin X-F, Kvitko B, He SY. Pseudomonas syringae: what it takes to be a pathogen.
619 *Nature Reviews Microbiology* **16**, 316-328 (2018).

620
621 16. Cheng C, Gao XQ, Feng BM, Sheen J, Shan LB, He P. Plant immune response to
622 pathogens differs with changing temperatures. *Nature Communications* **4**, 2530 (2013).

623
624 17. Zhu Y, Qian WQ, Hua J. Temperature Modulates Plant Defense Responses through
625 NB-LRR Proteins. *PLoS pathogens* **6** (2010).

626
627 18. Kumar SV*, et al.* Transcription factor PIF4 controls the thermosensory activation of
628 flowering. *Nature* **484**, 242-245 (2012).

629
630 19. Fu ZQ, Dong X. Systemic acquired resistance: turning local infection into global
631 defense. *Annu Rev Plant Biol* **64**, 839-863 (2013).

632
633 20. Wildermuth MC, Dewdney J, Wu G, Ausubel FM. Isochorismate synthase is required
634 to synthesize salicylic acid for plant defence. *Nature* **414**, 562-565 (2001).

635
636 21. Wang Y, Bao ZL, Zhu Y, Hua J. Analysis of Temperature Modulation of Plant
637 Defense Against Biotrophic Microbes. *Mol Plant Microbe In* **22**, 498-506 (2009).

638
639 22. Scott IM, Clarke SM, Wood JE, Mur LAJ. Salicylate accumulation inhibits growth at
640 chilling temperature in Arabidopsis. *Plant Physiology* **135**, 1040-1049 (2004).

23. Barah P, Jayavelu ND, Rasmussen S, Nielsen HB, Mundy J, Bones AM. Genome-scale cold stress response regulatory networks in ten Arabidopsis thaliana ecotypes. *Bmc Genomics* **14**, 722 (2013).

24. Yang SH, Hua J. A haplotype-specific Resistance gene regulated by BONZAI1 mediates temperature-dependent growth control in Arabidopsis. *The Plant cell* **16**, 1060-1071 (2004).

25. Alcazar R, Garcia AV, Parker JE, Reymond M. Incremental steps toward incompatibility revealed by Arabidopsis epistatic interactions modulating salicylic acid pathway activation. *Proceedings of the National Academy of Sciences of the United States of America* **106**, 334-339 (2009).

26. Huang X, Li J, Bao F, Zhang X, Yang S. A Gain-of-Function Mutation in the Arabidopsis Disease Resistance Gene RPP4 Confers Sensitivity to Low Temperature. *Plant Physiology* **154**, 796-809 (2010).

27. Zbierzak AM, Porfirova S, Griebel T, Melzer M, Parker JE, Dormann P. A TIR-NBS protein encoded by Arabidopsis Chilling Sensitive 1 (CHS1) limits chloroplast damage and cell death at low temperature. *Plant Journal* **75**, 539-552 (2013).

28. Stuttmann J. Arabidopsis thaliana DM2h (R8) within the Landsberg RPP1-like resistance locus underlies three different cases of EDS1-conditioned autoimmunity. *PLoS Genet* **12**, (2016).

29. Huot B, Yao J, Montgomery BL, He SY. Growth-Defense Tradeoffs in Plants: A Balancing Act to Optimize Fitness. *Molecular plant* **7**, 1267-1287 (2014).

30. Fan M*, et al.* The bHLH Transcription Factor HBI1 Mediates the Trade-Off between Growth and Pathogen-Associated Molecular Pattern-Triggered Immunity in Arabidopsis. *The Plant cell* **26**, 828-841 (2014).

31. Lozano-Duran R, Macho AP, Boutrot F, Segonzac C, Somssich IE, Zipfel C. The transcriptional regulator BZR1 mediates trade-off between plant innate immunity and growth. *Elife* **2**, (2013).

32. Karasov TL, Chae E, Herman JJ, Bergelson J. Mechanisms to Mitigate the Trade-Off between Growth and Defense. *The Plant cell* **29**, 666-680 (2017).

33. Wolinska J, King KC. Environment can alter selection in host-parasite interactions. *Trends in Parasitology* **25**, 236-244 (2009).

34. Berens ML, *et al.* Balancing trade-offs between biotic and abiotic stress responses through leaf age-dependent variation in stress hormone cross-talk. *Proceedings of the National Academy of Sciences of the United States of America* **116**, 2364-2373 (2019).

35. Bechtold U, *et al.* Constitutive salicylic acid defences do not compromise seed yield, drought tolerance and water productivity in the Arabidopsis accession C24. *Plant Cell and Environment* **33**, 1959-1973 (2010).

36. Deng YW, *et al.* Epigenetic regulation of antagonistic receptors confers rice blast resistance with yield balance. *Science* **355**, 962-965 (2017).

37. Campos ML, *et al.* Rewiring of jasmonate and phytochrome B signalling uncouples plant growth-defense tradeoffs. *Nature Communications* **7**, 12570 (2016).

38. Ariga H, *et al.* NLR locus-mediated trade-off between abiotic and biotic stress adaptation in Arabidopsis. *Nat Plants* **3**, 17072 (2017).

39. Horton MW, *et al.* Genome-wide patterns of genetic variation in worldwide Arabidopsis thaliana accessions from the RegMap panel. *Nature genetics* **44**, 212-216 (2012).

40. Tonsor SJ, Scott C, Boumaza I, Liss TR, Brodsky JL, Vierling E. Heat shock protein 101 effects in A. thaliana: genetic variation, fitness and pleiotropy in controlled temperature conditions. *Molecular Ecology* **17**, 1614-1626 (2008).

41. Huang WE, *et al.* Quantitative in situ assay of salicylic acid in tobacco leaves using a genetically modified biosensor strain of Acinetobacter sp ADP1. *Plant Journal* **46**, 1073-1083 (2006).

42. Marek G, Carver R, Ding YZ, Sathyanarayan D, Zhang XD, Mou ZL. A high-throughput method for isolation of salicylic acid metabolic mutants. *Plant Methods* **6**, 21 (2010).

43. Todesco M, *et al.* Natural allelic variation underlying a major fitness trade-off in Arabidopsis thaliana. *Nature* **465**, 632-U129 (2010).

44. Song JT, Koo YJ, Seo HS, Kim MC, Do Choi Y, Kim JH. Overexpression of AtSGT1, an Arabidopsis salicylic acid glucosyltransferase, leads to increased susceptibility to Pseudomonas gringae. *Phytochemistry* **69**, 1128-1134 (2008).

45. Miura K, *et al.* SIZ1 deficiency causes reduced stomatal aperture and enhanced drought tolerance via controlling salicylic acid-induced accumulation of reactive oxygen species in Arabidopsis. *Plant Journal* **73**, 91-104 (2013).

728 46. Cui H. A core function of EDS1 with PAD4 is to protect the salicylic acid defense
729 sector in Arabidopsis immunity. *New Phytol* **213**, 1802-1817 (2017).

730
731 47. Molina A, Hunt MD, Ryals JA. Impaired fungicide activity in plants blocked in
732 disease resistance signal transduction. *The Plant cell* **10**, 1903-1914 (1998).

733
734 48. Delaney TP, *et al.* A Central Role of Salicylic-Acid in Plant-Disease Resistance.
735 *Science* **266**, 1247-1250 (1994).

736
737 49. Cao H, Bowling SA, Gordon AS, Dong XN. CHARACTERIZATION OF AN
738 ARABIDOPSIS MUTANT THAT IS NONRESPONSIVE TO INDUCERS OF
739 SYSTEMIC ACQUIRED-RESISTANCE. *The Plant cell* **6**, 1583-1592 (1994).

740
741 50. Seren U, *et al.* GWAPP: A Web Application for Genome-Wide Association Mapping
742 in Arabidopsis. *The Plant cell* **24**, 4793-4805 (2012).

743
744 51. Kover PX, *et al.* A Multiparent Advanced Generation Inter-Cross to Fine-Map
745 Quantitative Traits in Arabidopsis thaliana. *PLoS genetics* **5**, (2009).

746
747 52. Mukhtar MS, *et al.* Independently evolved virulence effectors converge onto hubs in a
748 plant immune system network. *Science* **333**, 596-601 (2011).

749
750 53. Chen ZY, *et al.* Expression analysis of the AtMLO gene family encoding plant-
751 specific seven-transmembrane domain proteins. *Plant Mol Biol* **60**, 583-597 (2006).

752
753 54. Coego A, *et al.* The TRANSPLANTA collection of Arabidopsis lines: a resource for
754 functional analysis of transcription factors based on their conditional overexpression. *Plant*
755 *Journal* **77**, 944-953 (2014).

756
757 55. Nozue K, *et al.* Rhythmic growth explained by coincidence between internal and
758 external cues. *Nature* **448**, 358-U311 (2007).

759
760 56. Huang H, *et al.* PCH1 integrates circadian and light-signaling pathways to control
761 photoperiod-responsive growth in Arabidopsis. *Elife* **5**, (2016).

762
763 57. Galvao VC, Collani S, Horrer D, Schmid M. Gibberellic acid signaling is required for
764 ambient temperature-mediated induction of flowering in Arabidopsis thaliana. *Plant*
765 *Journal* **84**, 949-962 (2015).

766
767 58. Heidrich K, Tsuda K, Blanvillain-Baufume S, Wirthmueller L, Bautor J, Parker JE.
768 Arabidopsis TNL-WRKY domain receptor RRS1 contributes to temperature-conditioned
769 RPS4 auto-immunity. *Frontiers in plant science* **4**, 403 (2013).

770

59. Zhu WS, *et al.* Modulation of ACD6 dependent hyperimmunity by natural alleles of an Arabidopsis thaliana NLR resistance gene. *PLoS genetics* **14**, (2018).

60. Wang D, Pajerowska-Mukhtar K, Culler AH, Dong XN. Salicylic acid inhibits pathogen growth in plants through repression of the auxin signaling pathway. *Current Biology* **17**, 1784-1790 (2007).

61. Nozue K, *et al.* Network Analysis Reveals a Role for Salicylic Acid Pathway Components in Shade Avoidance. *Plant Physiology* **178**, 1720-1732 (2018).

62. Bechtold U, Ferguson JN, Mullineaux PM. To defend or to grow: lessons from Arabidopsis C24. *J Exp Bot* **69**, 2809-2821 (2018).

63. Velasquez AC, Oney M, Huot B, Xu S, He SY. Diverse mechanisms of resistance to Pseudomonas syringae in a thousand natural accessions of Arabidopsis thaliana. *New Phytologist* **214**, 1673-1687 (2017).

64. Panchal S, *et al.* Regulation of Stomatal Defense by Air Relative Humidity. *Plant Physiology* **172**, 2021-2032 (2016).

65. Zhang YL, Goritschnig S, Dong XN, Li X. A gain-of-function mutation in a plant disease resistance gene leads to constitutive activation of downstream signal transduction pathways in suppressor of npr1-1, constitutive 1. *The Plant cell* **15**, 2636-2646 (2003).

66. Cui HT, *et al.* Antagonism of Transcription Factor MYC2 by EDS1/PAD4 Complexes Bolsters Salicylic Acid Defense in Arabidopsis Effector-Triggered Immunity. *Molecular plant* **11**, 1053-1066 (2018).

67. Fournier-Level A, Korte A, Cooper MD, Nordborg M, Schmitt J, Wilczek AM. A Map of Local Adaptation in Arabidopsis thaliana. *Science* **334**, 86-89 (2011).

68. Brachi B, *et al.* Investigation of the geographical scale of adaptive phenological variation and its underlying genetics in Arabidopsis thaliana. *Molecular Ecology* **22**, 4222-4240 (2013).

69. Gunther T, Lampei C, Barilar I, Schmid KJ. Genomic and phenotypic differentiation of Arabidopsis thaliana along altitudinal gradients in the North Italian Alps. *Molecular Ecology* **25**, 3574-3592 (2016).

70. Chevance FFV, Hughes KT. Case for the genetic code as a triplet of triplets. *Proceedings of the National Academy of Sciences of the United States of America* **114**, 4745-4750 (2017).

71. Oh E, Zhu JY, Wang ZY. Interaction between BZR1 and PIF4 integrates brassinosteroid and environmental responses. *Nat Cell Biol* **14**, 802-U864 (2012).

72. Atwell S*, et al.* Genome-wide association study of 107 phenotypes in Arabidopsis thaliana inbred lines. *Nature* **465**, 627-631 (2010).

73. Chao DY*, et al.* Genome-Wide Association Studies Identify Heavy Metal ATPase3 as the Primary Determinant of Natural Variation in Leaf Cadmium in Arabidopsis thaliana. *PLoS genetics* **8**, (2012).

74. García AV. Balanced nuclear and cytoplasmic activities of EDS1 are required for a complete plant innate immune response. *PLoS Pathog* **6**, (2010).

75. Straus MR, Rietz S, Ver Loren van Themaat E, Bartsch M, Parker JE. Salicylic acid antagonism of EDS1-driven cell death is important for immune and oxidative stress responses in Arabidopsis. *Plant J* **62**, 626-640 (2010).

76. DeFraia CT, Schmelz EA, Mou ZL. A rapid biosensor-based method for quantification of free and glucose-conjugated salicylic acid. *Plant Methods* **4**, 4-28 (2008).

77. Czechowski T, Stitt M, Altmann T, Udvardi MK, Scheible WR. Genome-wide identification and testing of superior reference genes for transcript normalization in Arabidopsis. *Plant Physiology* **139**, 5-17 (2005).

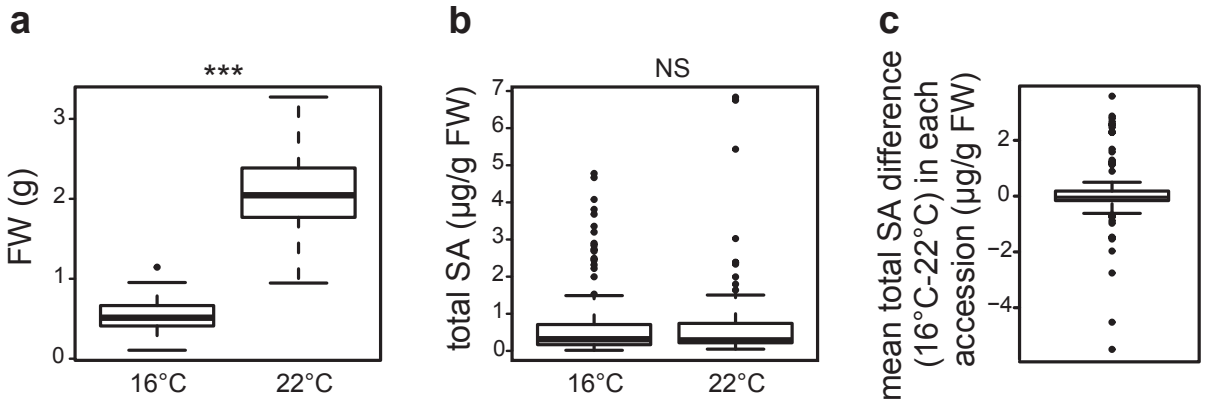

840

841 **Fig. 1**: Analysis of biomass and total SA levels in 105 *A. thaliana* accessions grown for 5
842 weeks at two temperature regimes (22°C and 16°C) reveals natural variation in SA
843 homeostasis in response to temperature. Data are represented as boxplots. **a)** Aboveground
844 fresh weight (FW) of plants grown at 16°C (n=420, four biological replicates) and 22°C
845 (n=315, three biological replicates). Statistical difference according to kruskal-wallis non
846 parametric test are indicated above the plot. **b)** Leaf total SA contents of plants grown at 16°C
847 (n=420) and 22°C (n=315). Statistical difference according to kruskal-wallis non parametric
848 test is indicated above the plot. **c)** Distribution of mean leaf total SA differences in accessions
849 between temperature regimes (n=105). Accessions with higher SA contents at 16°C than 22°
850 are at the positive side and accessions with higher SA contents at 22°C than at 16°C on the
851 negative side of the plot. Accessions with little or no change in SA contents in response to
852 temperature score around 0.

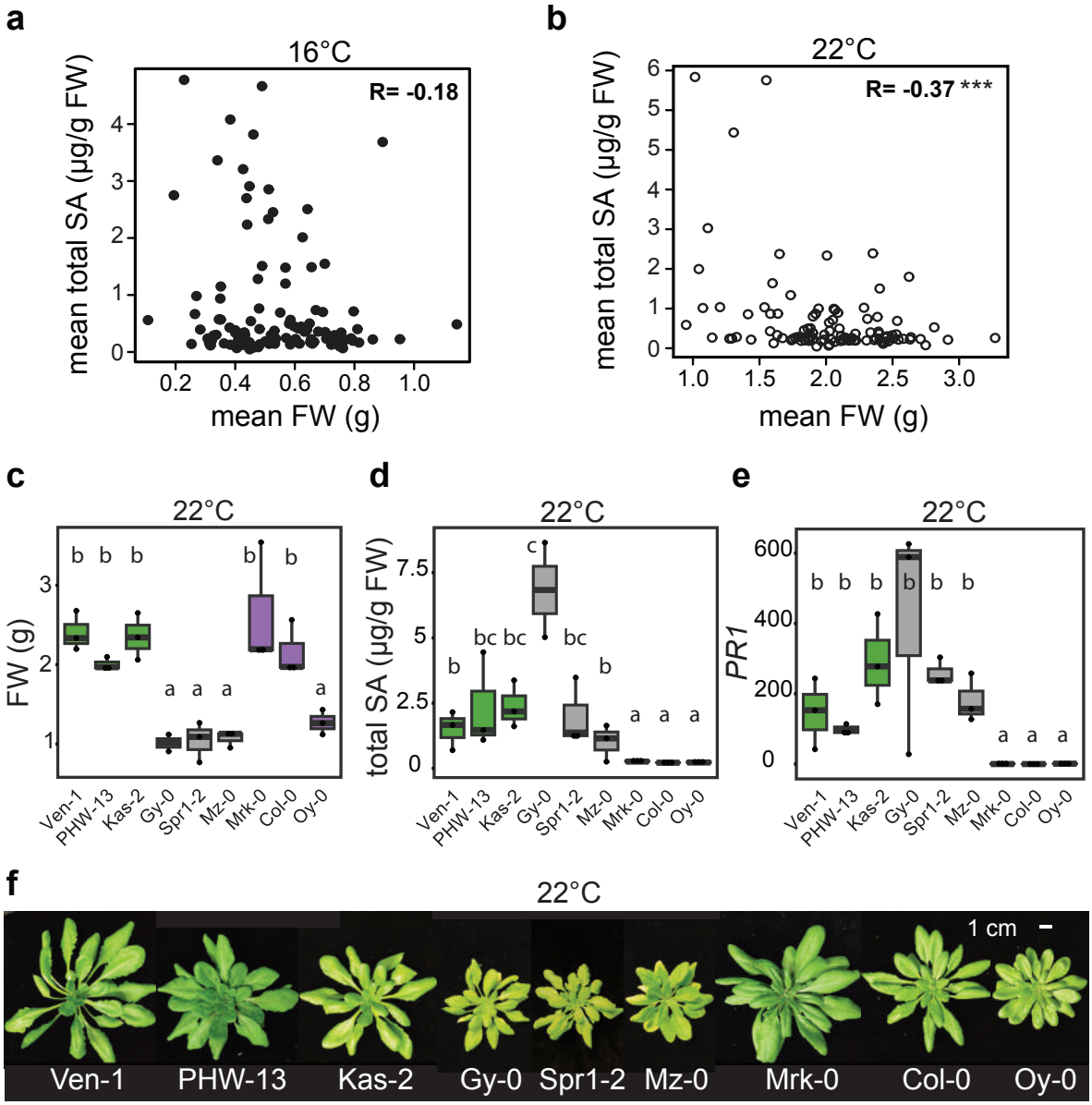

Fig. 2: Natural variation in growth - defense tradeoffs in *A. thaliana.* **a)** Scatterplot of mean above-ground fresh weight (FW) according to mean leaf total SA contents of 105 *A. thaliana* accessions grown for 5 weeks at 16°C. R= Pearson's correlation index. Data are from four biological replicates (t = -1.9184, df = 103, p-value = 0.05783). **b)** Scatterplot of mean above-ground FW according to mean leaf total SA contents of 105 *A. thaliana* accessions grown for 5 weeks at 22°C. R= Pearson's correlation index. Data are from three biological replicates (t = -4.0581, df = 103, p-value = 9.651e-05). **c)** Above-ground FW in 5-week-old plants of nine *A. thaliana* accessions grown at 22°C (n=3 biological replicates). Letters indicate significant differences after FDR multiple testing correction in one-way ANOVA. **d)** Leaf total SA contents in 5-week-old plants of nine *A. thaliana* accessions grown at 22°C (n=3 biological replicates). Letters indicate significant differences after FDR multiple testing correction in one-way ANOVA. Data was log(10) transformed for statistical analysis . **e)** Expression of *PR1* relative to *SAND* reference gene in 5-week-old plants of 9 *A. thaliana* accessions grown at 22°C (n=3 biological replicates). Letters indicate significant differences after FDR multiple testing correction in one-way ANOVA. Data was log(10) transformed for statistical analysis. **f)** Visual growth phenotypes of 5-week old *A. thaliana* accessions examined in c) to e).

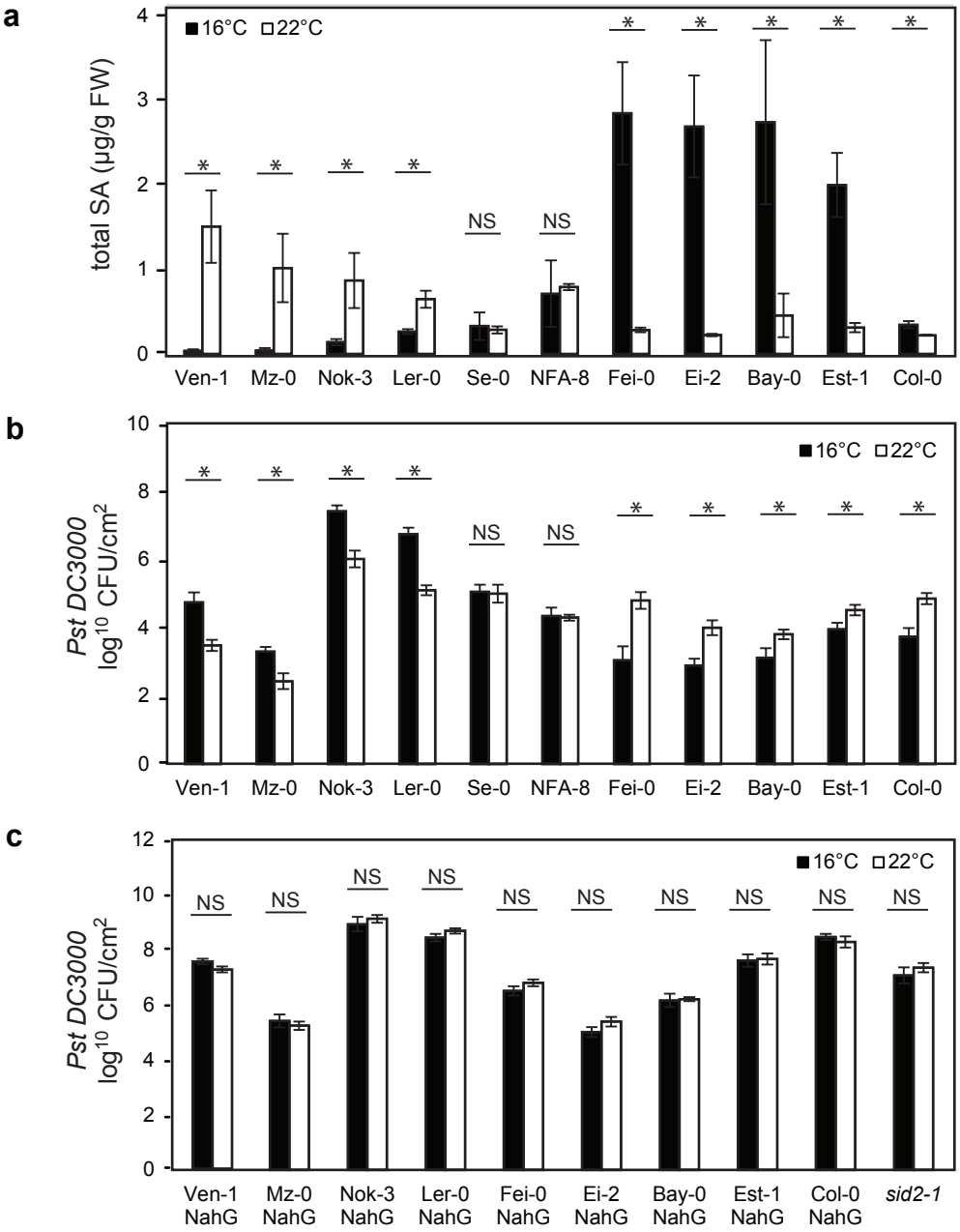

Fig. 3: Temperature-modulated SA accumulation impacts resistance to *Pst* DC3000. **a)** Leaf total SA content in 5-week-old plants of 11 *A. thaliana* accessions grown at 16°C (n=4 biological replicates) or 22°C (n=3 biological replicates). Significant differences between temperature regimes after kruskal-wallis non parametric test with p-values <0.05 are indicated with a star. Error bars represent standard error. **b)** Bacterial titres in leaves of 5-week-old plants of 11 *A. thaliana* accessions grown at 16°C or 22°C at 4 dafter spray-inoculation with *Pst* DC3000 (n=18, three biological replicates). Significant differences between temperatures after Student t-test with p-values < 0.05 are indicated on plot with a star. Error bars represent standard error. Day 0 sample measurements are shown in Fig. S5. **c)** Bacterial counts in leaves of 5-week-old plants of 11 SA-deficient (*NahG* transgenic) *A. thaliana* accessions grown at 16°C or 22°C, at 4 d after infection with *Pst* DC3000 (n=18 except for Ven-1 NahG where n=12, three biological replicates). Significant differences between temperatures after Student t-test with p-values < 0.05 are indicated with a star. Error bars represent standard error. Day 0 sample measurements are shown in Fig. S5.

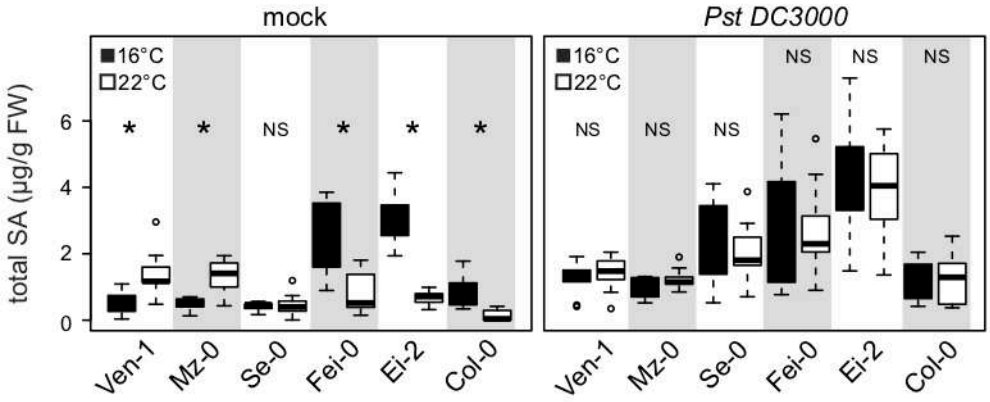

885

886 **Fig. 4:** Inducibility of total SA by *Pst DC3000* of leaves at 16°C and at 22°C. Leaf total SA
887 contents in 5-week old *A. thaliana* accessions with different temperature-modulated SA
888 contents were assessed at 24 h after spray-treatment with 10mM $MgCl_2$ (mock) or *Pst*
889 DC3000 (OD_{600}=0.15). Three individual plants per experiment were assessed per experiment
890 and three independent experiments performed (n=9). Significant differences between
891 temperatures after Student t-test with p-values <0.05 are marked with a star.

892

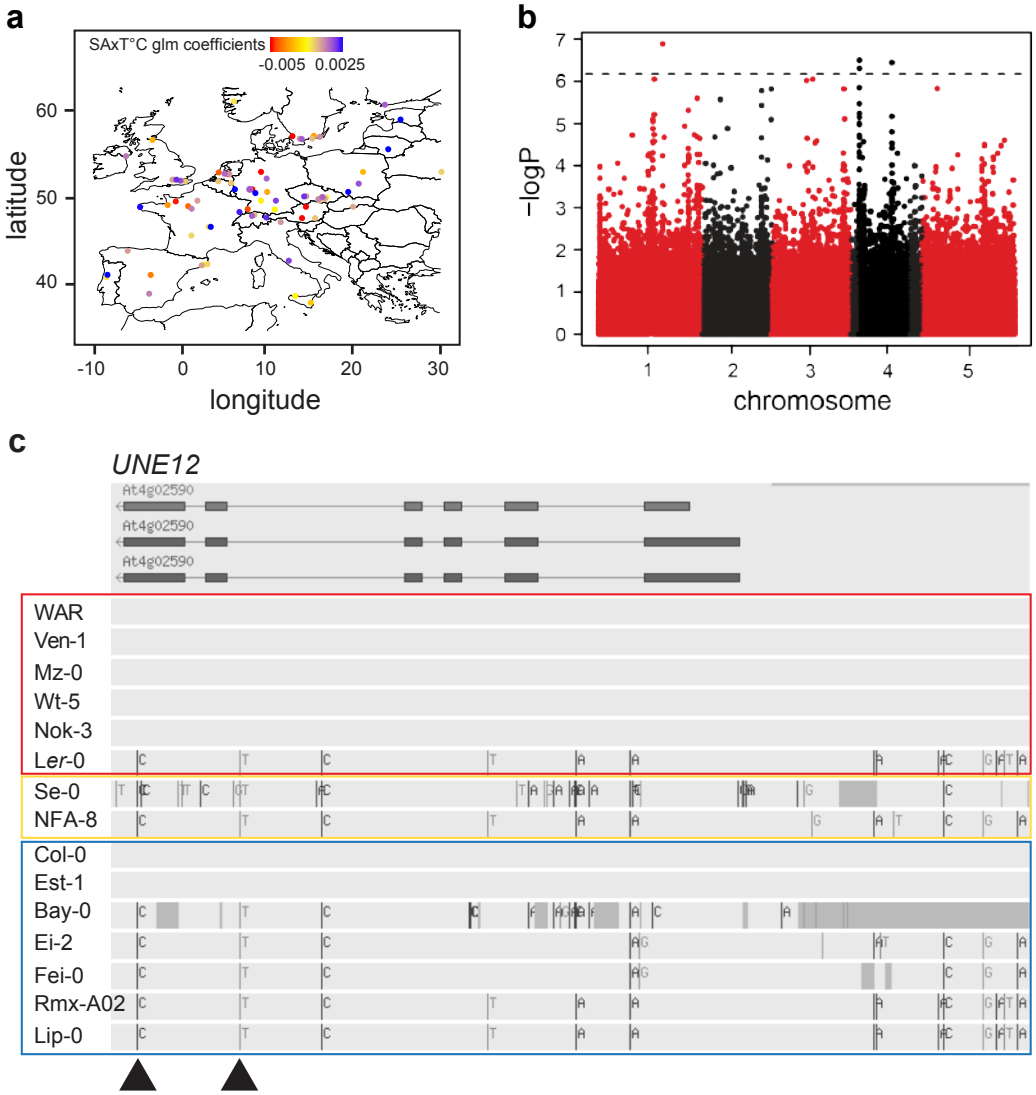

Fig. 5: Distribution and genetic architecture of SA regulation by temperature in *A. thaliana*. **a)** Geographical distribution of 78 *A. thaliana* accessions from Europe, representing 75% of phenotyped accessions. Dot colours indicate phenotypes of SA regulation by temperature according to coefficients of our glm model. Colour scale represents accessions displaying higher SA contents at 22°C than at 16°C in red, equal SA contents in yellow and higher SA contents at 16°C than at 22°C in blue. **b)** Manhatten plot of association mapping with 99 *A. thaliana* accessions for SA regulation by temperature according to GWAPP using the coefficients of our glm model. Each dot represents a single nucleotide polymorphism and the dashed horizontal line indicates significant linkage disequilibrium threshold after Bonferroni multiple testing correction. **c)** *UNE12* haplotypes according to Tair10 genome browser of accessions with extreme and intermediate total SA x T°C phenotypes. Colour blocks indicate phenogroups as displayed in phenotype distribution map in Fig 5a. Arrows indicate significant SNPs associated with total SA x T°C phenotype considered by GWAPP.

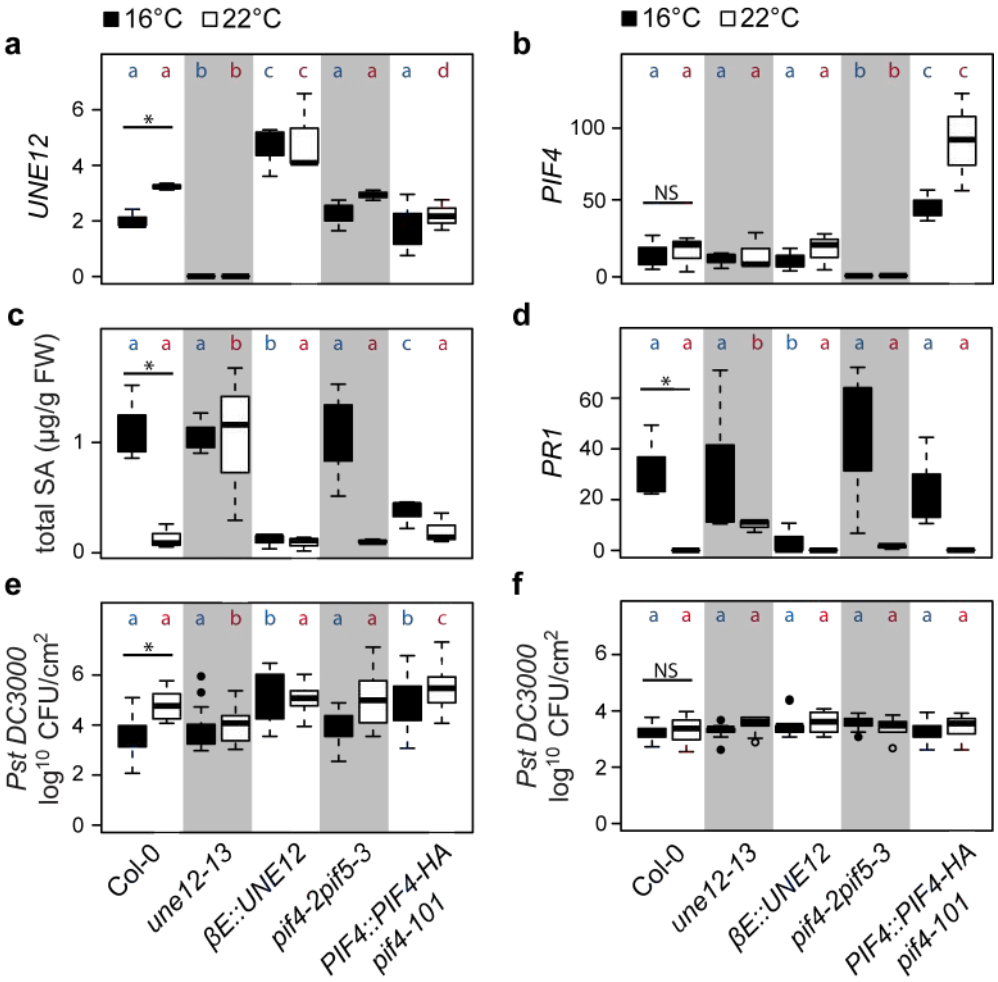

Fig. 6: Comparison of defence-related phenotypes in 5-week old Col-0, *UNE12* or *PIF4* mutants and transgenic lines, as indicated, grown at 16°C or 22°C. Data are represented as boxplots. Letters represent significant differences between genotypes after Tukey's multiple testing correction in one way ANOVA. Blue = 16°C, red = 22°C. **a)** *UNE12* expression relative to *SAND* reference gene in mature leaves of 5-week-old plants (n=3 biological replicates). **b)** *PIF4* expression relative to *SAND* mature leaves of 5-week-old plants (n=3 biological replicates). **c)** Total SA contents in mature leaves of 5-week-old plants (n=3 biological replicates). **d)** *PR1* expression relative to *SAND* in mature leaves of 5-week-old plants (n=3 biological replicates). **e)** *Pst* DC3000 growth in leaves at 4 d after spray inoculation (n=18 from 3 biological replicates). **f)** *Pst* DC3000 initial titres in leaves 4 h after spray inoculation (n=9 from 3 biological replicates).

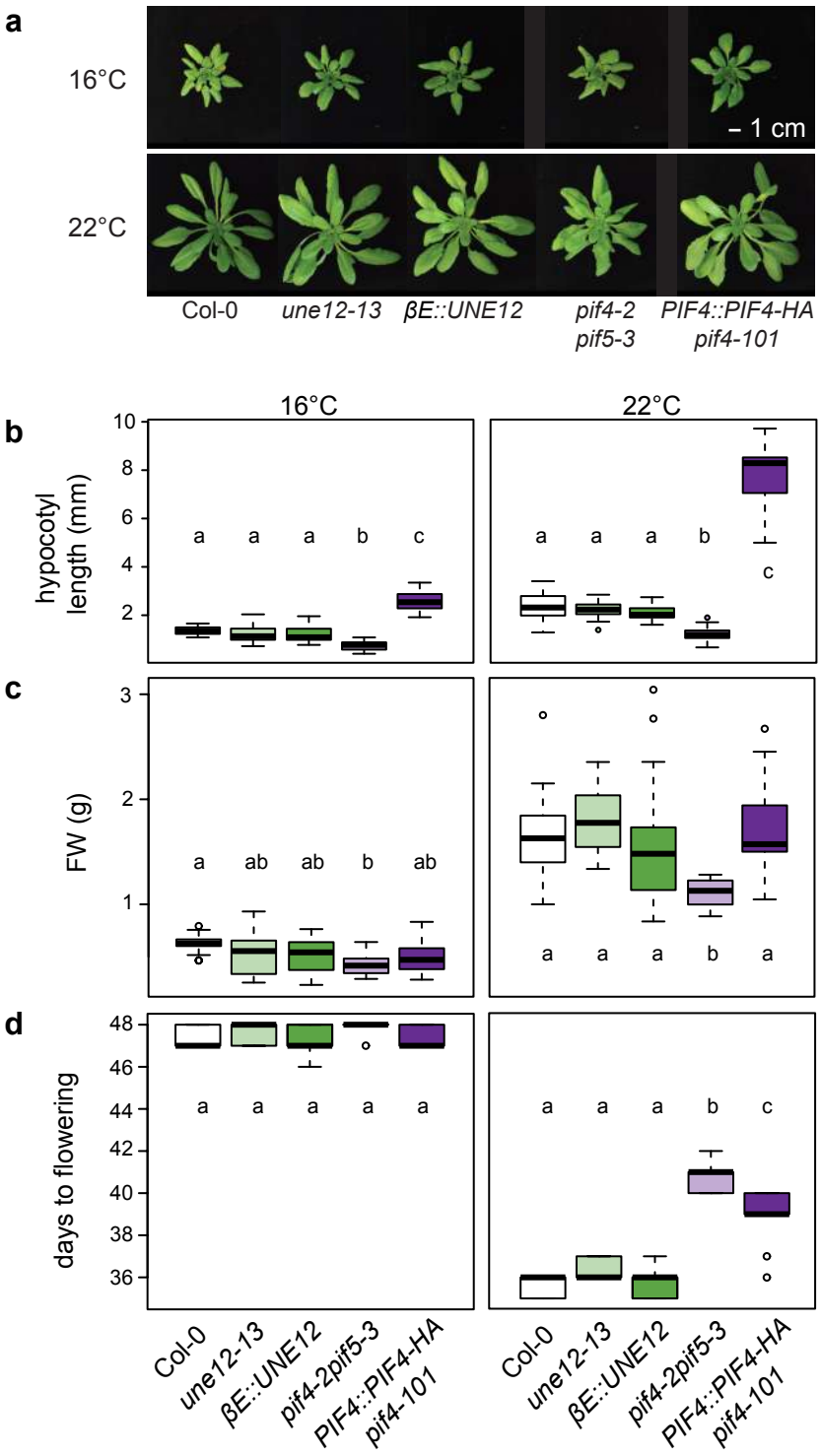

Fig. 7: Comparing developmental phenotypes of Col-0, *UNE12* and *PIF4* lines, as indicated, grown at 16°C or 22°C. Letters represent significant differences between genotypes after Tukey's multiple testing correction in one-way ANOVA. **a)** Visual phenotypes of 5-week-old plants. **b)** Hypocotyl lengths of seedlings 10 d after germination (n=15 from three biological replicates). **c)** Above-ground fresh weights of 5-week-old plants (n=14 from three biological replicates). **d)** Days to flowering (n=9 from three biological replicates).

927

928 **Supplementary material**

929 **Table S1**: Phenotypic data from 105 *A. thaliana* accessions used to assess natural variation of
930 biomass and total SA levels in response to temperature

931

932

933 **Table S2**: Correlation between above ground fresh weight and dry weight in 5-week-old *A.*
934 *thaliana* accessions grown at 22°C under controlled conditions

	replicate a		replicate b		replicate c	
accession	**R**	**p-value**	**R**	**p-value**	**R**	**p-value**
Bor-4	0,99	1,00E-07	0,99	6,20E-06	0,96	1,00E-04
C24	0,99	2,90E-07	0,99	9,30E-07	0,97	4,75E-05
Col-0	0,99	1,00E-09	0,99	2,70E-06	0,98	3,09E-02
Est-1	0,99	3,80E-06	0,98	1,90E-05	0,83	1,00E-02
Sha	0,99	2,80E-05	0,99	4,90E-08	0,92	1,00E-03
Ws-0	0,99	8,90E-08	0,99	4,90E-06	0,95	3,85E-08

Data collected from 6 *A. thaliana* accessions in 5 week-old plants (DF = 7). R= Pearson's correlation index.

935

936

937

938 **Table S3**: Genes in vicinity of SNPs highly associated with T°C-dependent total SA
939 homeostasis

chromosome	position	-log (P)	AGI	gene name	neighbouring genes
1	***18311139***	**6.88**	***At1g49470***	***unknown***	***tRNA, regulator of transcription luminidependens gene,***
4	***1129443***	**6.5**	***At4g02570***	***CUL1***	***NADH oxidored.***
4	***1134041***	**6.5**	***At4g02580***	***NADH-ubiquinone oxidoreductase 24kD subunit***	***CUL1, UNE12***
4	***1135657***	**6.5**	***At4g02580***	***NADH-ubiquinone oxidoreductase 24kD subunit***	***CUL1, UNE12***
4	***1146995***	**6.5**	***At4g02600***	***MLO1***	***UNE12, Trp synthase***
4	***10461125***	**6.44**	***At4g19120***	***ERD3***	***prot. kinase, unknown***
4	***1138019***	**6.29**	***At4g02590***	***UNE12***	***NADH-uboquinone oxidoreductase 24kD subunit, MLO1***
4	***1138410***	**6.29**	***At4g02590***	***UNE12***	***NADH-uboquinone oxidoreductase 24kD subunit, MLO1***
1	*15967192*	6.05	*At1g42525*	*unknown*	*ransposable element (TE), TE*
1	*28283354*	5.59	*At1g75380*	*AtBBD1*	*Sec14p-like prot., unknown*
2	*19096217*	5.81	*At2g46520*	*unknown*	*bHLH transcription factor, ARF11*
2	*16261705*	5.77	*At2g38950*	*transcription factor*	*At phosphate transporter 2, ERO2*
2	*4482275*	5.56	*At2g11240*	*TE*	*TE, transferase*
3	*11227279*	6.05	*At3g29265*	*TE*	*oxidoreductase, ubiquitin-prot. ligase*
3	*9398878*	6.01	*At3g25740*	*MAP1B*	*EDF3, Fbox prot.*
3	*20168050*	5.81	*At3g54470*	*unknown*	*Fbox prot., SKIP5*
3	*20176964*	5.81	*At3g54500*	*unknown*	*RNAPol II E, ERD4*
4	*1115823*	5.84	*At4g02540*	*unknown*	*thylakoid prot., unknown*
4	*1115996*	5.84	*At4g02540*	*unknown*	*thylakoid prot., unknown*
4	*1117210*	5.84	*At4g02540*	*unknown*	*thylakoid prot., unknown*
4	*1119896*	5.84	*At4g02541*	*unknown*	*unknown, unknown*
5	*4913335*	5.82	*At5g15150*	*homeobox 3 gene*	*aldose 1-epimerase, bHLH prot.*

Table S2: Loci significantly associated with T°C-dependent total SA homeostasis after Bonferroni correction are represented in bold

940

941

942

943 **Table S4**: Primer list for RT-qPCR

AGI	sense	gene	sequence
AT2G28390	Fw	SAND	AACTCTATGCAGCATTTGATCCACT
AT2G28390	Rv	SAND	TGATTGCATATCTTTATCGCCATC
AT2G14610	Fw	PR1	TTCTTCCCTCGAAAGCTCAA
AT2G14610	Rv	PR1	AAGGCCCACCAGAGTGTATG
AT4G02590	Fw 3'	UNE12	TCTAACGATGGGACTGAACG
AT4G02590	Rv 3'	UNE12	CTACTGTGGAGGATTGTTCTC
AT4G02590	Fw 5'	UNE12	TGGCTAGTAACAACCCTCAC
AT4G02590	Rv 5'	UNE12	AATCCTCCGTCAACTCCAGA
AT2G43010	Fw	PIF4	CGGAGTTCAACCTCAGCAGT
AT2G43010	Rv	PIF4	ACCGGGATTGTTCTGAATTG

944

945

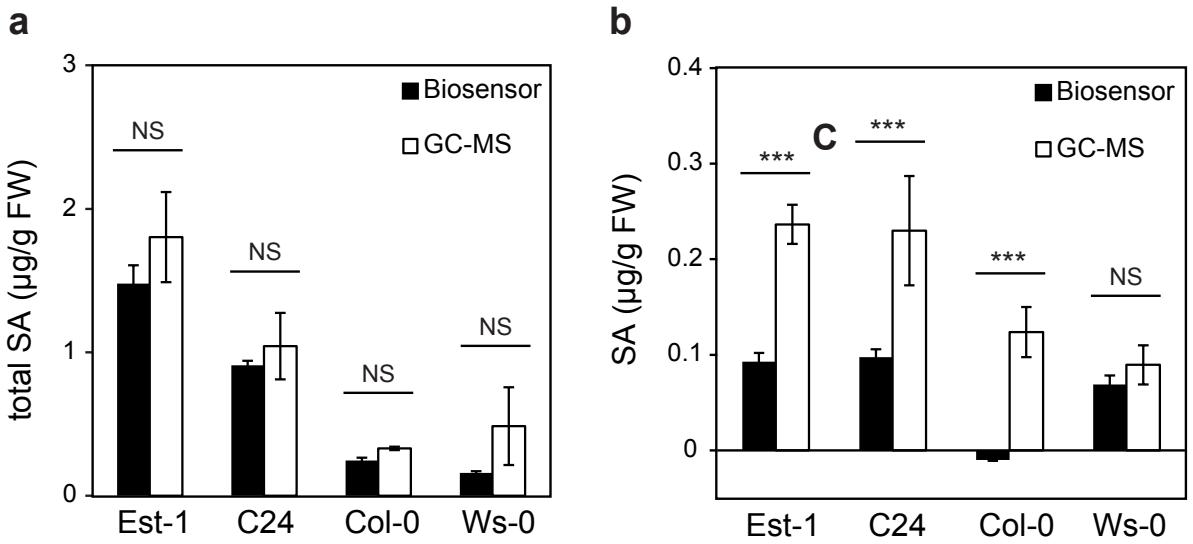

Fig. S1: Comparing *Acinetobacter* biosensor-based method and GC-MS analysis for measuring total and free SA contents in *A. thaliana* leaves of 7-week-old plants. **a)** Total SA in four *A. thaliana* accessions with contrasting SA contents grown at 22°C (n=5). Significant differences between methods after Student t-test are indicated with a star on plot. **b)** Free SA in four *A. thaliana* accessions with contrasting SA contents grown at 22°C (n=5). Significant differences between methods after Student t-test are indicated on plot.

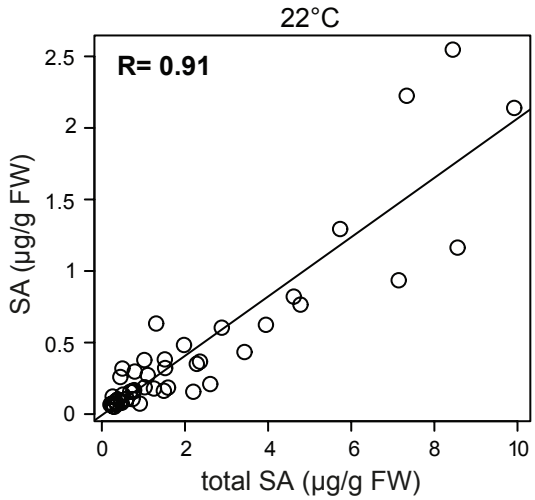

954

955 **Fig. S2:** Correlation of total SA and free SA contents measured by GC-MS in 15 *A. thaliana*
956 accessions in three biological replicates. Plants were 5-week-old when sampled and grown at
957 22°C. R= Pearson's correlation index (t = 14.365, df = 43, p-value < 2.2e-16).

958

959

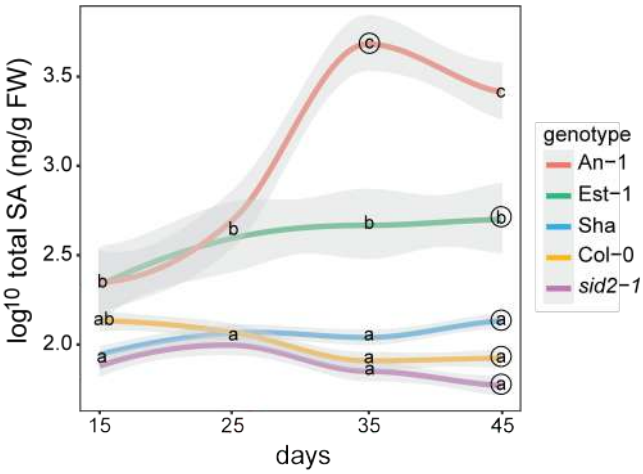

960

961 **Fig. S3:** Total SA contents measured over developmental time in five *A. thaliana* accessions
962 or mutants with contrasting SA contents (n=12 from three biological replicates except for 15 d
963 time point where n=2). Letters indicate significant differences after Tukey's multiple testing
964 correction in one-way ANOVA. Circles indicate time point at which 100% plants were
965 flowering. Grey shadows indicate standard error.

966

967

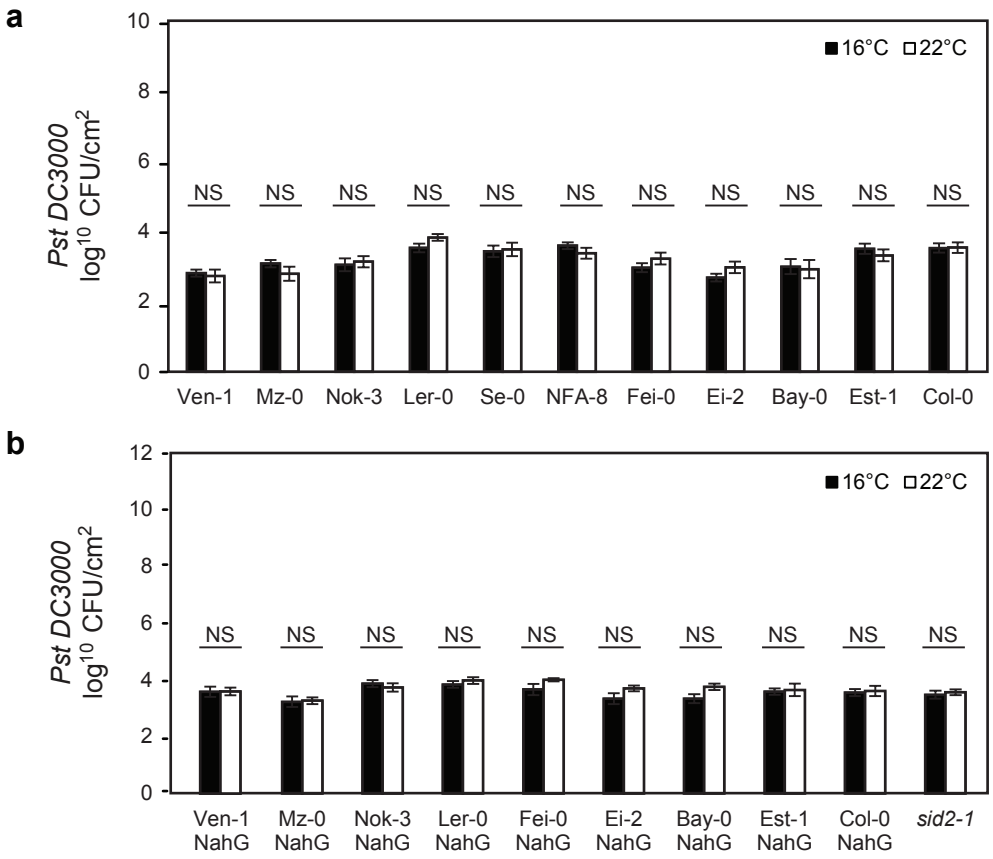

968

969 **Fig. S4:** Bacterial titres in leaves of *A. thaliana* accessions 4 h after spray inoculation with *Pst*
970 DC3000. **a)** Bacteria-inoculated 5-week-old plants of 11 *A. thaliana* accessions, as indicated,
971 grown at 16°C or 22°C (n=9, three biological replicates). Significant differences between
972 temperatures after Student t-test with p-values < 0.05 are indicated on plot with a star. Error
973 bars represent standard error. **b)** Bacteria-inoculated 5-week-old plants of 10 SA-deficient *A.*
974 *thaliana* accessions grown at 16°C or 22°C (n=9 from 3 biological replicates except for Ven-1
975 where n=6). Significant differences between temperatures after Student t-test with p-values <
976 0.05 are indicated on plot with a star. Error bars represent standard error.

977

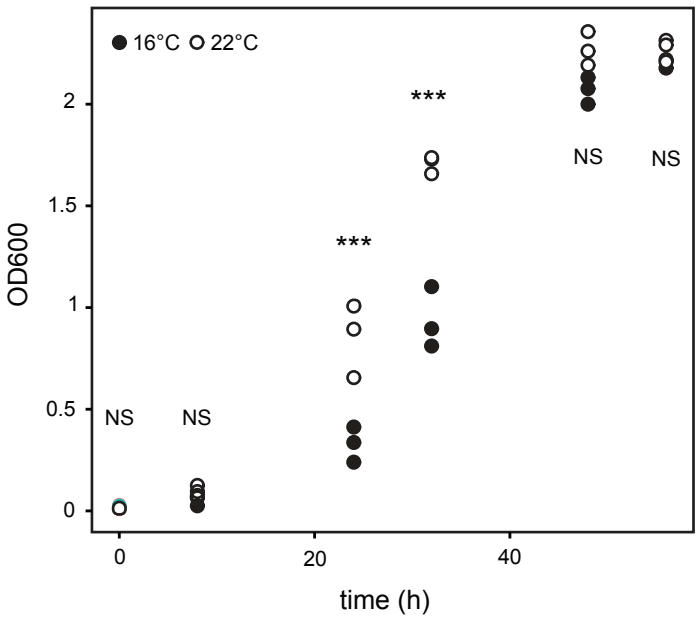

978

979 **Fig. S5:** *Pst* DC3000 growth time course on minimal liquid medium. Bacteria were measured
980 by optical density (OD_{600}) increase over 56 h in M9 minimal salt medium with sorbitol at
981 16°C (black) and 22°C (white) (n=3 from three biological replicates). Significant differences
982 after Student t-test are represented with stars.

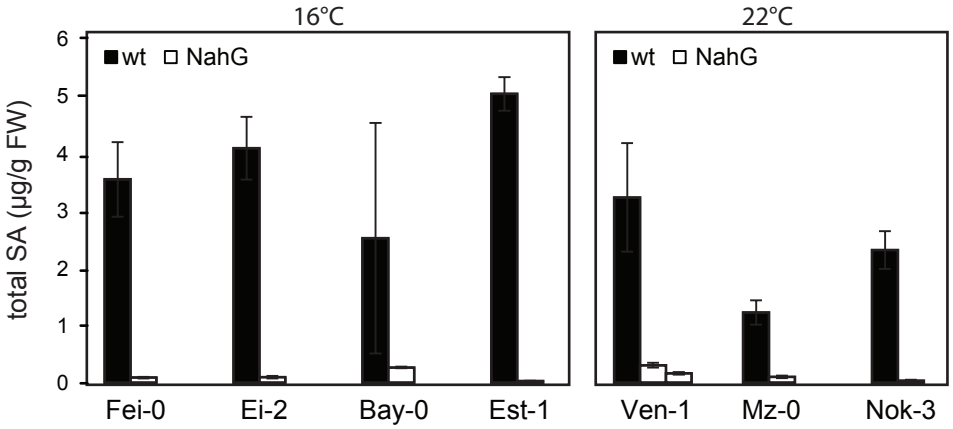

983

984 **Fig. S6:** Leaf total SA contents in 5-week-old *A. thaliana* accessions (black) and transgenic *A.*
985 *thaliana* accessions transformed with a bacterial *NahG* gene (white). Lines were phenotyped
986 in the environment in which the parental line displayed highest SA accumulation to ensure
987 full SA depletion (n=3 from 3 biological replicates). Error bars represent standard error.

988

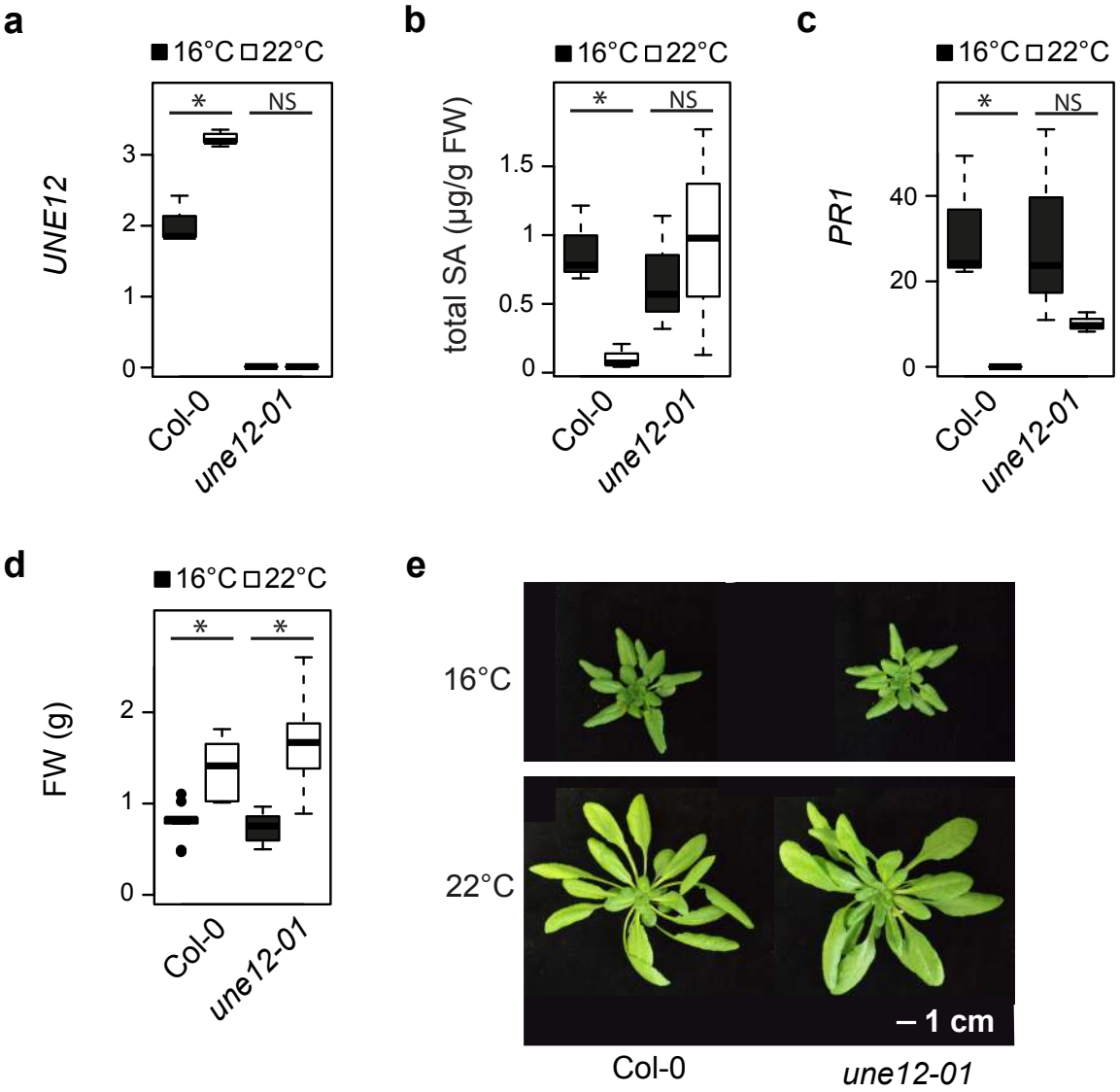

Fig. S7: Comparison of phenotypes between Col-0 and *une12-01* T-DNA insertion line in 5-week-old plants grown at 16°C and 22°C. Data are represented as boxplots. **a)** *UNE12* expression relative to *SAND* reference gene in mature leaves (n=3 from biological replicates). Significant differences between temperatures after Student t-test with p-values < 0.05 are indicated on plot with a star. **b)** Total SA contents in mature leaves (n=3 from biological replicates). Significant differences between temperatures after Student t-test with p-values < 0.05 are indicated on plot with a star. **c)** *PR1* expression levels relative to *SAND* in mature leaves (n=3 from biological replicates). Significant differences between temperatures after Student t-test with p-values < 0.05 are indicated on plot with a star. **d)** Above-ground fresh weight (n=3 from 3 biological replicates). Significant differences between temperature regimes after Student t-test with p-values < 0.05 are indicated on plot with a star. **e)** Visual phenotypes of lines at 16°C and 22°C.